AR-010-403

Prediction of Radar Pulse Envelope Distortion due to Tropospheric Propagation

Marina Ozerova

DSTO-TN-0125

DEPARTMENT OF DEFENCE

DEFENCE SCIENCE AND TECHNOLOGY ORGANISATION

Prediction of Radar Pulse Envelope Distortion due to Tropospheric Propagation

Marina Ozerova

Electronic Warfare Division
Electronics and Surveillance Research Laboratory

DSTO-TN-0125

ABSTRACT

This project is a part of research into the detection of radar signals at ranges well beyond the horizon by exploiting the effect of tropospheric scattering. A result of this work is a program written in C language which enables the distortion of the envelope of a given radar pulse, which occurs as a result of propagating over any path by tropospheric scattering, to be predicted.

APPROVED FOR PUBLIC RELEASE

DEPARTMENT OF DEFENCE

DEFENCE SCIENCE AND TECHNOLOGY ORGANISATION

Published by

DSTO Electronics and Surveillance Research Laboratory
PO Box 1500
Salisbury South Australia 5108

Telephone: (08) 8259 5555
Fax: (08) 8259 6567

AR-010-403
December 1997
APPROVED FOR PUBLIC RELEASE

Prediction of Radar Pulse Envelope Distortion due to Tropospheric Propagation

EXECUTIVE SUMMARY

The objective of the work described in this report is to investigate the possibilities of detecting radar transmissions from very long range by means of tropospheric scatttering.

The propagation of radio waves via the troposphere occurs as a result of a scattering mechanism which takes place in the volume of the tropospheric medium where the beams of the transmitting and receiving antennas overlap.

Radar signals which propagate via the troposphere will have a distorted pulse envelope shape due to the difference in the transit time between the shortest and longest paths from the transmitter to the receiver via the extremities of the scattering volume. The extent of the distortion will depend on the pulse duration compared to the time difference between propagation via the longest and shortest paths.

The main objective of the work described in this report was to predict the distortion of the pulse envelope shape of radar signals after propagation via the troposphere. In order to optimise the detection of tropospheric scattered radar signals it is desirable to be able to predict this distortion to enable a better matched filter to be designed.

The procedure adopted is to assume that the variations to the pulse shape result from the spatial distribution of the scattering and the scattering mechanism is equivalent to the reflection of the signal from a large number of point reflectors randomly distributed within the scattering volume.

Author

Marina Ozerova
Wide Area Surveillance Division

Marina Ozerova recently joined DSTO as a Professional Officer Class 1 in Wide Area Surveillance Division although the work described in this report was done in Electronic Warfare Division prior to her appointment. Marina was born in Russia and graduated from the Physics Faculty of Nizhny Novgorod State University in 1987. She defended her project on low temperature deposition of A_2B_6 semiconductors using high frequency plasma thermo-decomposition of $Cd(CH_3)_2$ and $Te(CH_3)_2$ metal organic compounds widely used in infra-red detectors. Marina emigrated to Australia in 1993 and has since become an Australian Citizen. After arriving in Australia she undertook a number of work experience jobs to help adapt to the Australian work environment and to improve her command of English. Work experience included working as a Physicist for the Department of Mines and Energy, the Radiation Protection Branch of the S.A. Health Commission and, finally, with Electronic Warfare Division of the DSTO.

Contents

1. Introduction

The problem of scattering of electromagnetic waves in the troposphere attracts considerable attention from scientists and engineers. The phenomenon related to long-range atmospheric propagation of short waves beyond the limits of the "radio horizon" is known to be one of the least developed subjects of this kind.

Thus, the propagation of radio waves via the troposphere occurs as a result of the poorly understood mechanism of scattering which takes place in the volume of space where the beams of the transmitting and receiving antennas overlap.

The goal of this project was not to dwell on all the numerous problems associated with the use of radio scattering for the purpose of long range communication. Instead, the main objective of the current project were to predict the distortion of the pulse envelope shape of radar signals after propagation via the troposphere. The ability to predict the pulse envelope will enable a better matched filter to be designed for detecting the signals.

Radar signals which propagate via the troposphere will have a distorted pulse envelope shape if the difference in the transit time between the shortest and longest paths from the transmitter to the receiver, via the extremities of the scattering volume, is comparable with the pulse duration and in most instances this will be the case. In order to optimise the detection of tropospheric scattered radar signals it is desirable to be able to predict the pulse envelope distortion that will occur.

The area of our interest is in estimating the variations to the pulse shape and since this envelope shape distortion will not result from the scattering mechanism itself but from the spatial distribution of the scattering, it should be possible to calculate the likely effect by assuming the scattering mechanism is equivalent to the reflection of the signal from a large number of point reflectors distributed within the scattering volume.

As can be seen from Figure 1, if the elevation and azimuth beam shapes of the transmitting and receiving antennas are known, then we could calculate the signal strength and relative phase at the receiver for some nominal transmitter power and a nominal cross section reflector situated at any given point within the scattering volume. It is also possible to calculate the transit time between transmission and reception of this reflected signal.

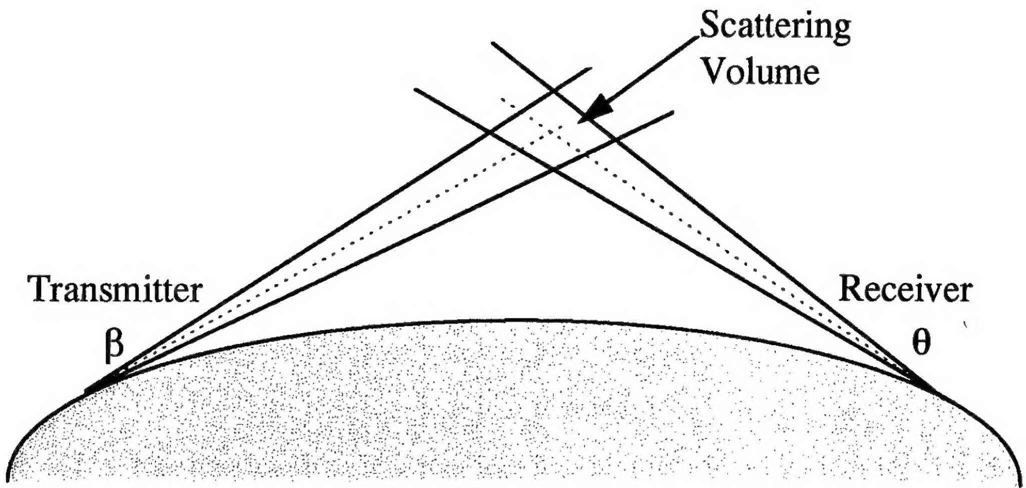

Figure 1: Scattering volume.

It is reasonable to assume that the envelope shape of the signal reflected from a point reflector will be identical to the envelope shape of the transmitted signal. Applying this condition to a large number of identical point reflectors distributed throughout the scattering volume and summing all the individual signals, taking into account the transit time delay of the amplitude envelope and the phase of each signal, then it should be possible to construct the probable amplitude profile of a troposcattered signal for any given transmitted signal envelope shape.

In this project we will not take into account the scattering phenomenon itself, i.e. attenuation, depolarisation and volume scattering effects leading to troposcatter losses. Only a brief theoretical introduction of these effects will be given. Results of computations of troposcatter losses employing known empirical approaches, i.e. NBS, Yeh, Rider etc. were presented in [5].

However, it is believed that the results of the current project which considers the change in the envelope shape due to spatial distribution of the reflectors inside the scattering volume, could be coupled with the results of earlier work [5] in future tasks in order to estimate the combined effect.

2. Radio scattering in the troposphere

This section is a brief introduction and overview of the theory of propagation of radio waves via the troposphere.

2.1 Interaction processes in the troposphere

There are a number of possible mechanisms whereby radiowaves can interact with the lower atmosphere to produce scattering, these include:

- absorption and dispersion in atmospheric gases (oxygen, water vapour and minor constituents);
- scattering from atmospheric turbulence and scintillation;
- scattering and absorption in populations of hydrometeors (including anisotropic effects, forward scatter, back scatter, and scattering at arbitrary angles);
- scattering and absorption in sand and dust particle populations;
- refraction and reflection in stable atmospheric layers;
- thermal emission from hydrometeors and atmospheric gases.[1]

2.2 Theory of scattering and absorption

Attenuation, depolarization and volume scattering of radiowaves due to atmospheric particles are phenomena, which severely limit the performance of telecommunication systems.

Currently, mainly frequencies below 20 GHz are used by communication systems although the use of some millimetre wave frequencies where high absorption occurs has been advocated in the literature for short range secure links.

The basic theory describing different models for attenuation, depolarization and volume scattering is the theory for single-particle scattering. Particle scattering effects become more severe with higher frequencies. This is aggravated by the increasing effect of small particles, such as liquid droplets, which are present in great numbers in the atmosphere.

The problem of single and multiple scattering has been discussed by many authors. Some approaches have different interpretations of formulae and different ways to derive them.

Let us introduce just one model - single scattering approximation, which was described in Reference [3]. Here, the author considered a random medium illuminated by a transmitter. A part of the transmitted wave was scattered by the randomness of the medium and this scattered wave was detected by a receiver (Figure 2).

There was considered a volume δV in the random medium. It was assumed that the randomness of the medium was so slight that the wave incident on δV was almost equal to the incident wave in the absence of the random medium.

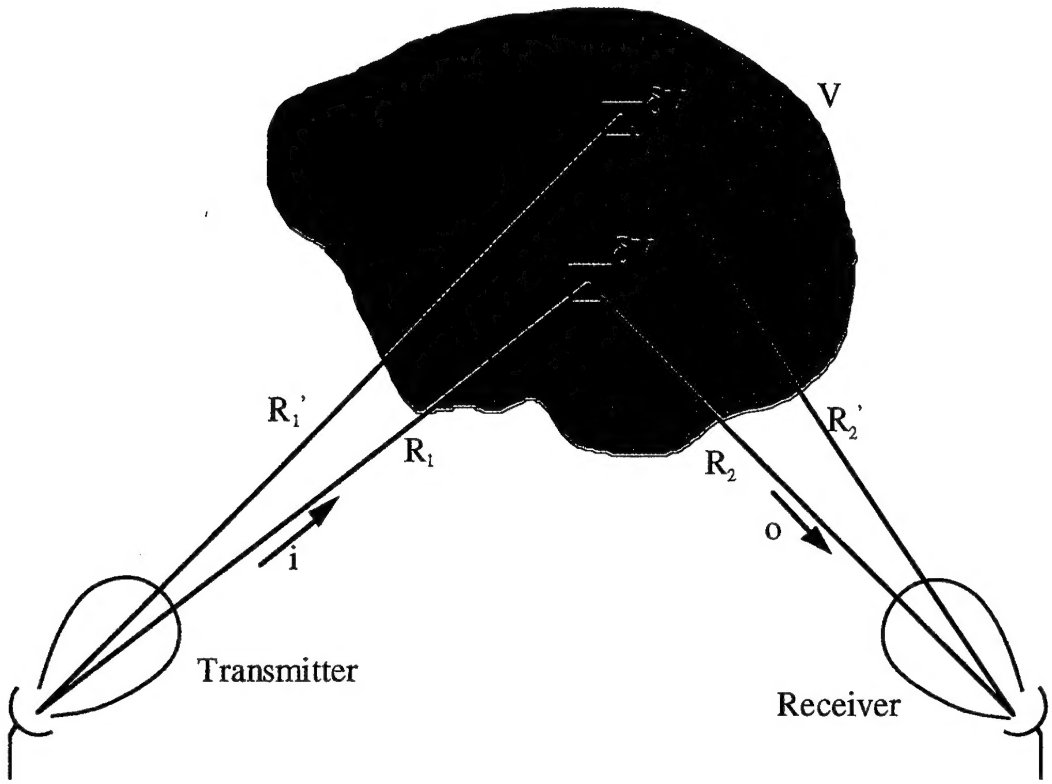

Figure 2: Geometry showing transmitter, receiver and random medium.

It was described by the amount of scattered power due to the random medium in δV in terms of the equivalent scattering cross section per unit volume $\sigma(0, I)$, then the received power P_r is given by the radar equation

$$P_r \,/\, P_t = \lambda^2 G_t(i) G_r(0)\; \sigma(0,i)\delta V / \;(4\pi)^2 R_1^2 R_2^2 \quad , \qquad (1)$$

where P_t - transmitted power

G_t, G_r - gain functions of the transmitter and receiver antennas in the directions of i and -0.

The basic scattering theory must be reviewed in order to find the limitations of its applicability to electromagnetic wave problems.

The theory of single and multiple scattering has been discussed in References [1, 2, 3, 4]. At this time, no references could be found that treat the basic scattering theory, as applied to communication systems, in a completely consistent way. This makes it difficult to understand the scattering theory [1].

2.3 Application of the theory of radio scattering in the troposphere to beam communication

Booker and Gordon [4] describe in their work the experiments made in the Caribbean Sea in 1945. The goal of these experiments was to explore the radio consequences of the evaporation-duct that exists at the ocean surface. As a result of this project it was discovered that, at any rate under some circumstances, field strength well beyond the horizon decreases with distance more slowly than could be expected on any existing theory. The wavelength used was 9 cm in this experiment. They found that the unexpectedly high field strengths obtained at long range on 9 cm were not due to duct propagation, and, accounting for the rather violent fading associated with them, it was suggested that a scattering mechanism was involved.

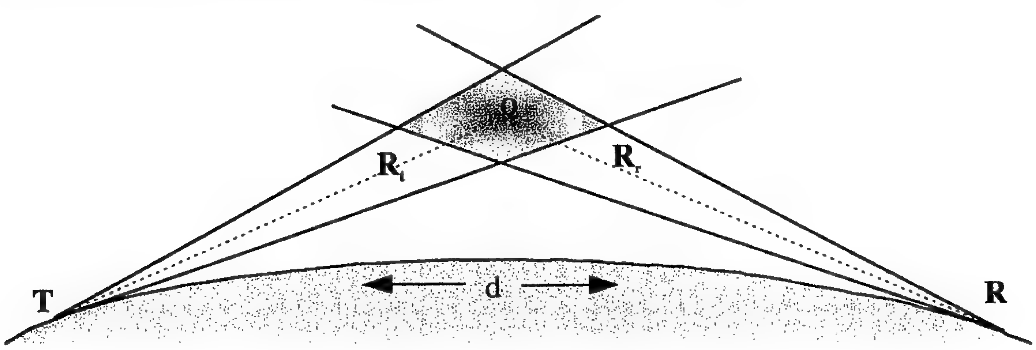

Figure 3: Antennas beams.

Booker and Gordon considered transmission from point T to point R at distance d round the curved surface of the earth by means of beamed antennas pointed more or less at each other as indicated in Figure 3. It was assumed that there were no ducts and that as far as ordinary reflection is concerned propagation was orthodox. It was supposed that both antennas were pointed horizontally at their respective locations, and that their axes lay in the vertical plane through T and R. For simplicity it was considered that the T and R antennas were identical. It was found that if the transmitter and receiver are omnidirectional, scattering is in general important from nearly the whole of the atmosphere above the horizons of both transmitter and receiver. However, in practice, both transmitter and receiver antennas usually have some directivity, and scattering is then important only in the region of atmosphere where the transmitting and receiving beams overlap.

As a result of the Caribbean experiments the following conclusions were made:

1. The modified scale of turbulence is expected to decrease with height above the earth's surface.

2. The theory of atmospheric scattering seems to predict a decrease of scattered field strength with distance that is too low to agree with the observation, in fact the scattering almost certainly decreases with height in most practical cases.

3. The height of the important scattering volume increases with the increase of distance between transmitter and receiver. An associated decrease of the modified scale of atmospheric turbulence would cause the scattering signal received to decrease more rapidly with the increase of range than for a uniformly turbulent atmosphere.

4. The same theory which is used for calculating the scattering signal at long distances may also be used in most cases for calculating the fading range at shorter distances.

3. Practical Procedure

First of all, it is necessary to emphasise that, because of the diverse nature of the problem, various approximations should be employed to obtain useful results. Therefore, some useful approximation techniques applicable to a variety of different situations will be presented in this project.

1. We will assume that the transmitter and receiver beam shapes are effectively rectangular.

2. We assign the transmitter to be at the origin ($x = 1$, $y = 0$) of a two dimensional coordinate system and the receiver to be on the x axis at a point that can be calculated from the great circle distance between the transmitter and receiver sites on the earth surface.

3. We assume both transmitter and receiver beam width to be the same.

4. Then we need to calculate the inclination of the transmitter and receiver antenna beams from the x axis, so that it is possible to calculate the x, y coordinates of the intersecting volume.

5. Next, it is necessary to calculate the coordinates of an array of point reflectors which were initially assumed to be regularly spaced within the intersecting volume although this was later extended to include a uniform density random distribution.

6. For each of the points in the array we then calculate the path length between transmitter and receiver via each point and hence determine the transmit time for each point reflected signal. Because we are interested only in the differences, we subtract the mean transit time from the actual transit time to obtain the delta transit time.

7. Since the signal which is assumed to be reflected from the reflector at each point starts from the transmitter with the same phase, we must now calculate the relative RF phase of each reflected signal by dividing the path length via each point reflector by the free space wavelength of the RF signal and discarding the integer part.

8. Since we have initially chosen to assume a rectangular beam shape and that the path difference from each point reflector will only differ by a small percentage we now assume that all the signals reflected from the point reflectors have the same (unity) amplitude profile.

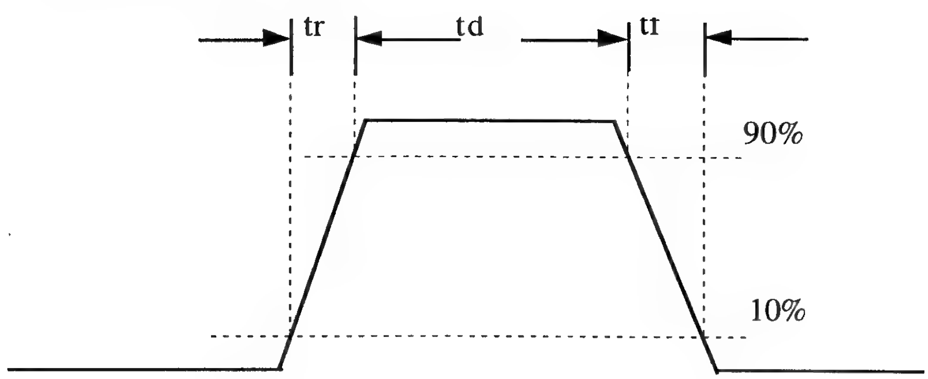

Figure 4: Pulse shape.

9. Now we define a suitable transmitter amplitude profile (pulse shape) by introducing three character-parameters, namely rise time t_r, fall time t_f, and duration t_d.

10. Finally, we produce a temporal plot of the resulting troposcattered waveform shape by doing a vector sum of all the point reflector outputs at each of a large number of time increments encompassing the pulse width and the range of delta transit time. The above is illustrated in Figure 4, and expressed more formally in the following equations:

$$\mathbf{A} = \sum(\mathbf{a_i} \cos\varphi_i + \mathbf{j}\ \mathbf{a_i} \sin\varphi_i), \tag{2}$$

where A - complex amplitude of the resulting envelope signal,

a_i - amplitude of initial envelope signal

$j = \sqrt{-1}$

$\varphi_i = (\nu l_i/c - \text{Integer}[\nu l_i/c])\, 2\pi$

φ_i - the phase of a signal reflected by point "i" from scattering volume,

ν - RF frequency in MHz,

c - the light speed in vacuum in [km/s]'

l_i - the length of the path from the transmitter to receiver via point "i" in [km].

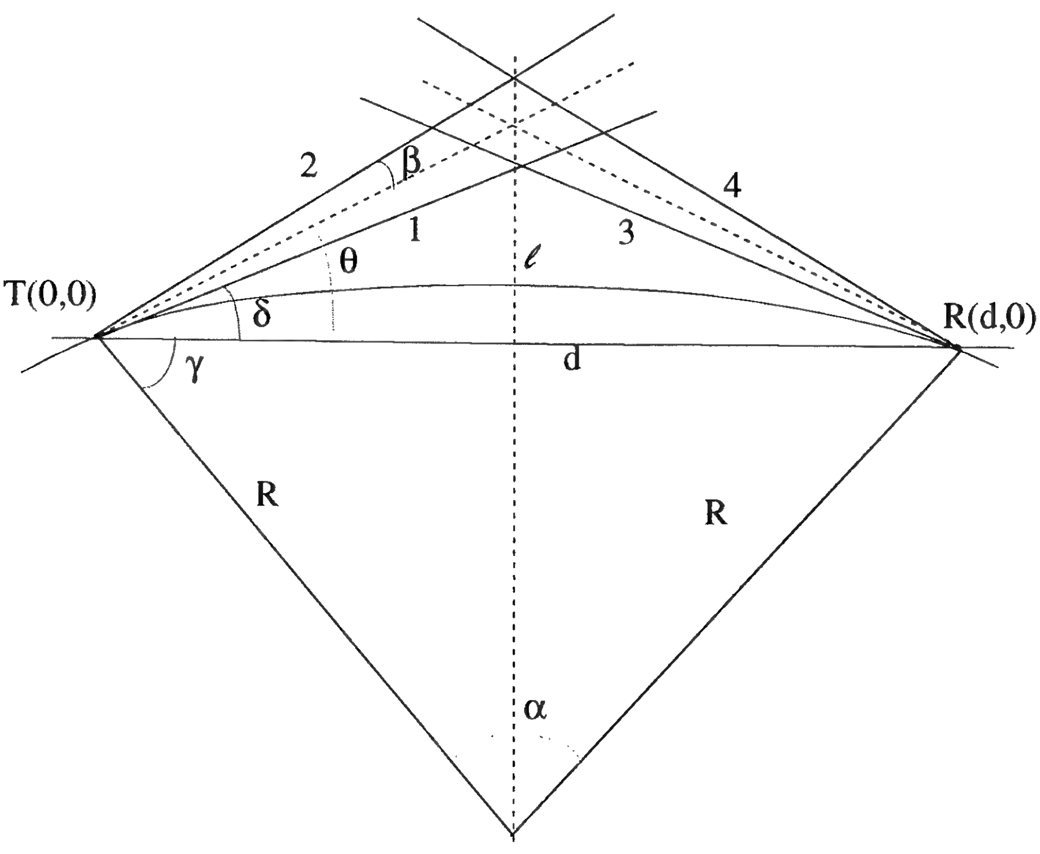

Figure 5: Geometry of beam intersection region.

$$y = \tan(\theta - \beta)\, x \qquad \text{(equation for line 1)} \tag{3}$$

$$y = \tan(\theta + \beta)\, x \qquad \text{(equation for line 2)} \tag{4}$$

Assumption $\theta_1 = \theta_2 = \theta$

$\beta_1 = \beta_2 = \beta$

$y = -\tan[\theta - \beta]\, x + b$

$0 = -\tan[\theta - \beta]\, d + b$

$d \tan[\theta - \beta] = b$

$$\mathbf{y = d\tan[\theta - \beta] - \tan[\theta - \beta]\, x} \quad \text{, (equation for line 3)} \tag{5}$$

$$\mathbf{y = d\tan[\theta + \beta] - \tan[\theta + \beta]\, x} \quad \text{, (equation for line 4)} \tag{6}$$

$$\mathbf{\tan[\theta - \beta]\, x = d\tan[\theta - \beta] - \tan[\theta - \beta]\, x} \quad , \tag{7}$$

$$\mathbf{2\tan[\theta - \beta]\, x = d\tan[\theta - \beta]} \quad , \tag{8}$$

$$\mathbf{x = d/2} \quad , \tag{9}$$

where

R - effective radius of Earth (4/3 physical radius)

β - the half beam width angle

l - the distance between the transmitter and the receiver

ϕ - the elevation angle of transmitter

n - number of points

$l = R\alpha$

$$\mathbf{d^2 = 2R^2 - 2R^2\cos\alpha = 2R(R - R\cos\alpha)} \quad , \tag{10}$$

$$\mathbf{d = \sqrt{2R(R - R\cos\alpha)}} \quad , \tag{11}$$

$$\gamma = (\pi - \alpha)/2 \quad , \tag{12}$$

$$\delta = \pi/2 - \gamma = \pi/2 - \pi/2 + \alpha/2 = \alpha/2 \quad , \tag{13}$$

$$\theta = \phi + \delta \quad , \tag{14}$$

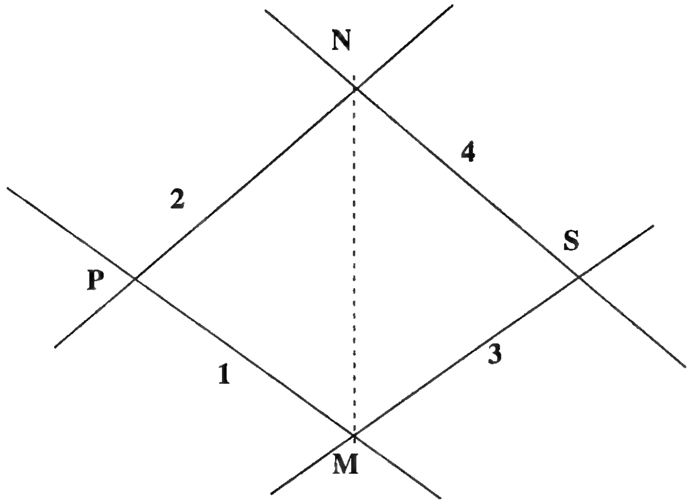

Figure 6: Scattering region.

We have equations for lines 1, 2, 3 and 4.

The ordinate of point N (y coordinate of N) is the maximum y value of the point to be distributed to the area.

The y coordinate of M is the minimum of y coordinate.

In the program the user specifies the numbers of rows, r and the spacing between the rows is Δ.

$$\Delta = \text{distance } NM/r \quad , \tag{15}$$

We know coordinates for the point N. N is specified by (x_N, y_N). Take the y coordinate and decrease it's value by Δ, i.e. $y_N - \Delta$.

From Equation 2 substitute $y_N - \Delta$ for y and solve for x. This gives us the first point of the first row - point N.

To get the next point, the coordinate will be ($x_N + \Delta$, $y_N - \Delta$). To find the maximum value of x put $y_N - \Delta$ into the equation 4 and solve x

While all this is being done, i.e. when each point is determined, we can at this time calculate the distance from transmitter to the receiver via the point. If the coordinates of the point are (x_P, y_P) then the distance from the transmitter to the receiver is

$$D = \sqrt{((x_P - x_T)^2 + (y_P - y_T)^2)} + \sqrt{((x_P - x_R)^2 + (y_P - y_R)^2)} \quad , \tag{16}$$

where x_T, y_T - coordinates of the transmitter,

x_R, y_R - coordinates of the receiver,

which are $(x_T, y_T) = (0, 0)$

$(x_R, y_R) = (d, 0)$

4. Operation

The software was developed and runs on an IBM PC and is written in Borland, Turbo C++, version 1.00. The plotting macros require the use of Excel, version 5.0. This section describes how the software can be operated.

4.1 Installation

- **pulse_d.exe, pulse_e.exe** and **pulse_r.exe** files should be installed in **c:\tc\bin** directory
- **pulse_d.xls, pulse_e.xls and pulse_r.xls** files in any directory

4.2 Execution

To obtain a plot of the reflection point distribution:

- run **pulse_d.exe** in DOS;
- save output to a file called **result_d.txt;**
- when finished computations, open **pulse_d.xls** in Excel;
- run the program in "Execute" Sheet of **pulse_d.xls** workbook.

To obtain a table of data and a plot of the pulse after reflection from a uniform array of points:

- run pulse_e.exe in DOS;
- save output to a file called result_e.txt;
- when finished computations, open pulse_e.xls in Excel;
- run the program in "Execute" Sheet of pulse_e.xls workbook

To obtain a table of data and a plot of the pulse after reflection from a random array of points:

- run pulse_r.exe in DOS;
- save output to a file named result_r.txt;
- when finished computations, open pulse_r.xls in Excel;
- run the program in "Execute" Sheet of pulse_r.xls workbook.

Note that the programs pulse_e.xls and pulse_r.xls are identical except for the result file accessed and the labels on the resulting curves.

5. Conclusions

1. Software for computing the modulation envelope after propagation of a given radar signal via the troposphere accounting for the effect of spatial distribution of point reflectors in the scattering volume has been designed and tested.

At this stage, the propagation model is based on point reflectors in a single plane having vertical and horizontal directions with two types of distribution, namely, equidistantly spaced and randomly spaced with uniform density. Elevation angles of both transmitter and receiver were chosen to be equal, as well as their beamwidth angles.

2. The Turbo C++ executable file allows one to plot resulting graphs on the screen and save the data in text format.

A special program was designed in Visual Basic for Excel, which can automatically read the data from the text file generated in Turbo C++ and then plot the graph of envelope amplitude versus time.

[Note that, with hindsight, it would have been much easier for users if the whole program had been designed in Visual Basic. In this case, a computation could be realised by striking one key either on keyboard or on the mouse.]

3. Analysis of the results of computations of radar pulse envelope distortion due to tropospheric propagation have shown (Appendix 1, 2):

- pulse shape envelope does change significantly with beamwidth and elevation angle as might be expected since these parameters determine the distance between the shortest and longest paths via the reflection points;
- with uniform distribution there is some evidence of an interference pattern, which is smoothed out to a large degree with a random distribution.

4. The next steps in developing the current model describing radar pulse envelope distortion are envisaged to be:

- extending the analysis to a three dimensional case;
- introducing a vertical variation in the density of the random distribution of reflecting points to reflect the likely variation resulting from the change in density of the troposphere with height;
- introducing some randomness and vertical variation in the amplitude of the reflection from each reflecting point;
- since real radars that we might wish to detect frequently employ a vertical fan shaped ($cosec^2$) beam, which is unlikely to be the best beam shape to use on the receiver, a new model is needed to take into account different values of beam width for the transmitting and receiving antennas.

6. Acknowledgments

This work was done in Electronic Warfare Division under a Technical Support Services contract and the author is grateful for the access to the DSTO library and other facilities that were made available.

The author would like to gratefully acknowledge the contribution from Dr A.Kulessa for the help and advice, he gave me while I was doing this project. Also the author wishes to express her thanks to Mr R. Lindop for help received on the same topic.

7. References

1. Brussurd, G., P.A. Watson, 1995. "Atmospheric Modeling and Millimetre Wave Propagation", Chapman & Hall, London.

2. Tatarski, V.I., 1961. "Wave Propagation in a Turbulent Medium", McGraw-Hill, New York.

3. Ishimaru, A., 1978, Volume 1, 2. "Wave Propagation and Scattering in Random Media", Academic Press, New York.

4. Booker, H.G.,W.E. Gordon, " A Theory of Radio Scattering in the Troposphere". (Proc. Inst. Radio Engrs. 38, 401 (1951))

5. Ozerova, M. "Troposcatter Loss Project" (Internal EWD Working Paper, DSTO, Salisbury, 1997).

Appendix A: Computations of Radar Pulse Envelope Distortion for Uniform Distribution

Grid with uniform distribtion of knots

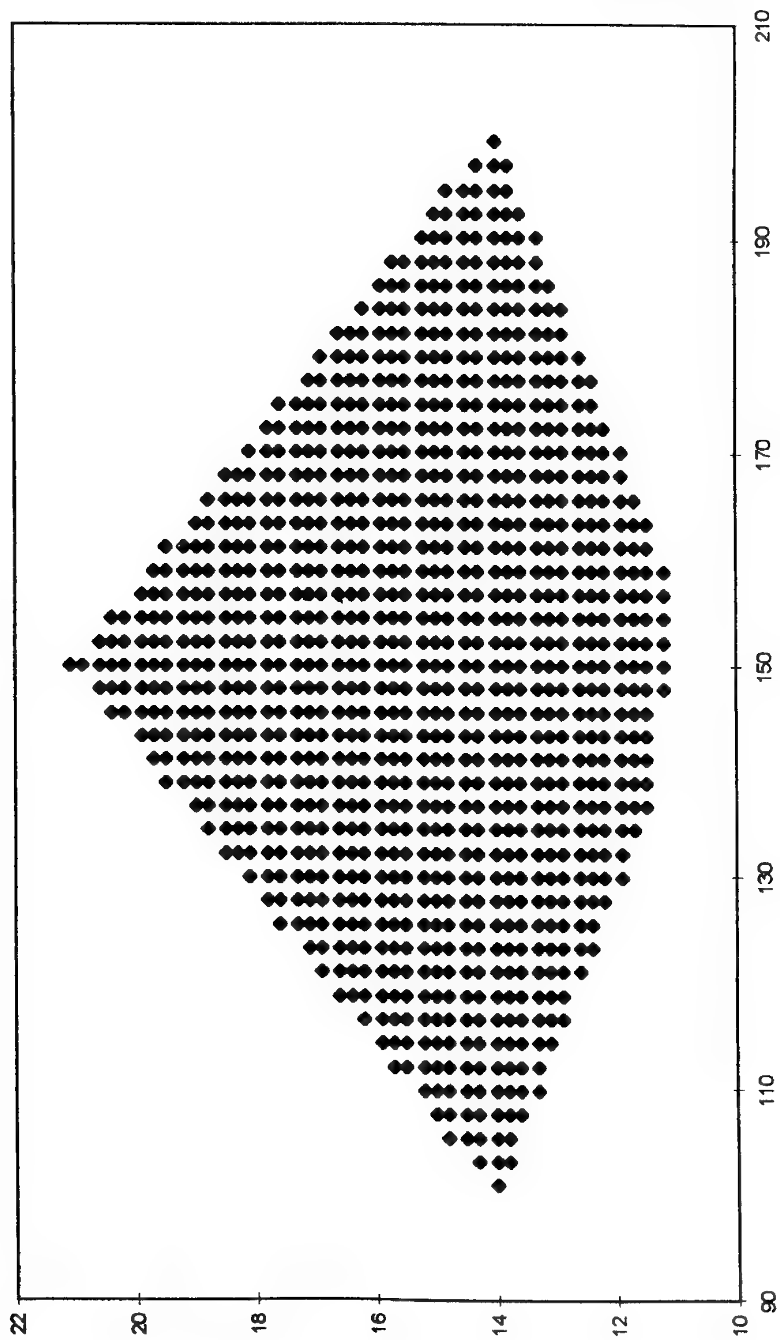

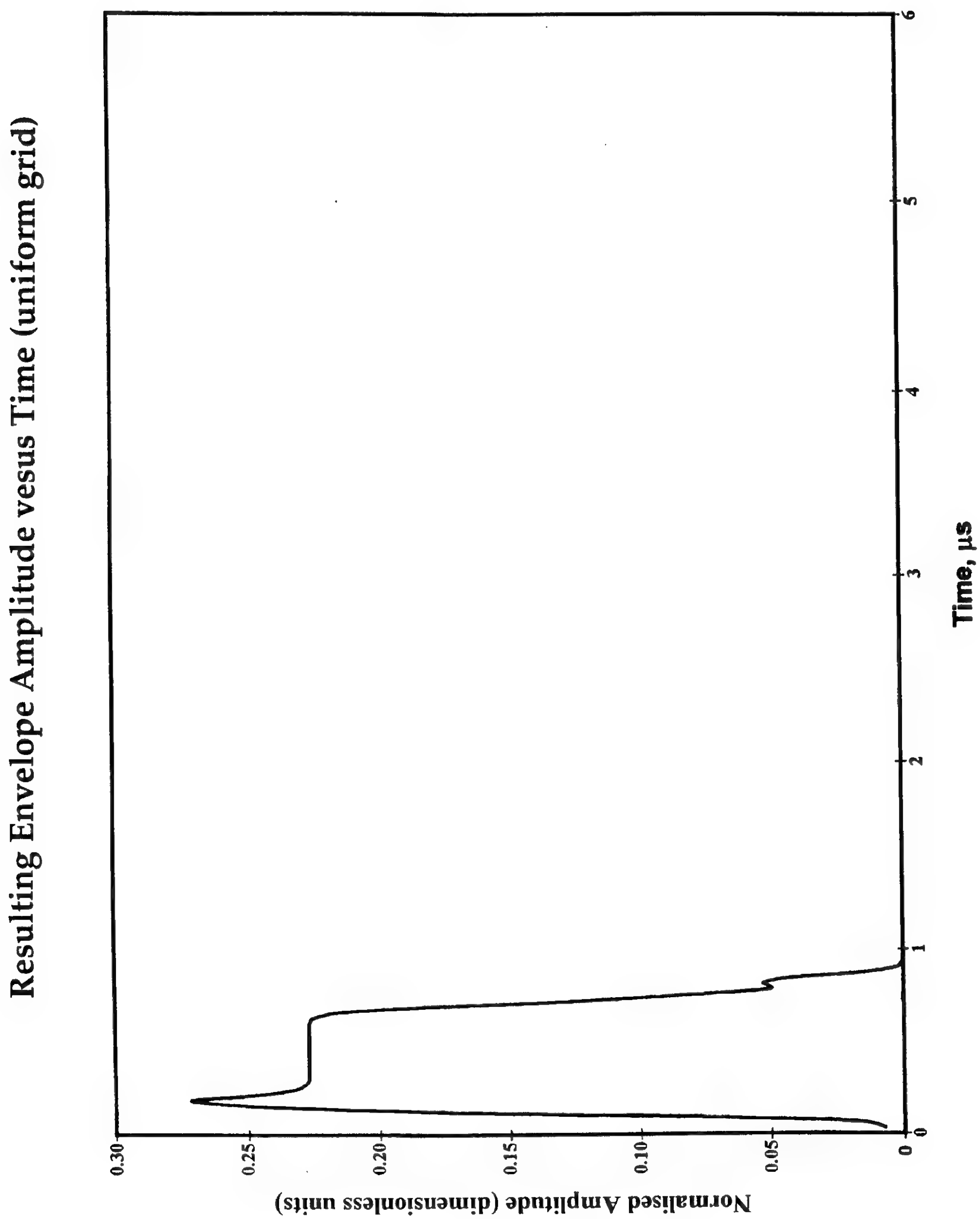
Resulting Envelope Amplitude vesus Time (uniform grid)
Normalised Amplitude (dimensionless units)
Time, µs
0
0.05
0.10
0.15
0.20
0.25
0.30
0
1
2
3
4
5
6

Beamwidth angle beta (degrees):	1.2
Great circle distance l (km):	300
Elevation angle phi (degrees):	0.7
Number of knots inside the scattering volume n:	1000
Operating frequency (MHz):	2830
Pulse rise time (μs):	0.1
Pulse width (μs):	0.5
Pulse fall time (μs):	0.15

i	Time[i]	Amplitude (arbitrary units)		i	Time[i]	Amplitude (arbitrary units)		i	Time[i]	Amplitude (arbitrary units)		i	Time[i]	Amplitude (arbitrary units)		i	Time[i]	Amplitude (arbitrary units)	
		Initial	Resulting			Initial	Resulting			Initial	Resulting			Initial	Resulting			Initial	Resulting
1	0.03	0.3	0.733	43	1.29	0	0	85	2.55	0	0	127	3.81	0	0	169	5.07	0	0
2	0.06	0.6	1.645	44	1.32	0	0	86	2.58	0	0	128	3.84	0	0	170	5.1	0	0
3	0.09	0.9	7.693	45	1.35	0	0	87	2.61	0	0	129	3.87	0	0	171	5.13	0	0
4	0.12	1	17.316	46	1.38	0	0	88	2.64	0	0	130	3.9	0	0	172	5.16	0	0
5	0.15	1	24.379	47	1.41	0	0	89	2.67	0	0	131	3.93	0	0	173	5.19	0	0
6	0.18	1	27.143	48	1.44	0	0	90	2.7	0	0	132	3.96	0	0	174	5.22	0	0
7	0.21	1	25.031	49	1.47	0	0	91	2.73	0	0	133	3.99	0	0	175	5.25	0	0
8	0.24	1	23.353	50	1.5	0	0	92	2.76	0	0	134	4.02	0	0	176	5.28	0	0
9	0.27	1	22.825	51	1.53	0	0	93	2.79	0	0	135	4.05	0	0	177	5.31	0	0
10	0.3	1	22.686	52	1.56	0	0	94	2.82	0	0	136	4.08	0	0	178	5.34	0	0
11	0.33	1	22.686	53	1.59	0	0	95	2.85	0	0	137	4.11	0	0	179	5.37	0	0
12	0.36	1	22.686	54	1.62	0	0	96	2.88	0	0	138	4.14	0	0	180	5.4	0	0
13	0.39	1	22.686	55	1.65	0	0	97	2.91	0	0	139	4.17	0	0	181	5.43	0	0
14	0.42	1	22.686	56	1.68	0	0	98	2.94	0	0	140	4.2	0	0	182	5.46	0	0
15	0.45	1	22.686	57	1.71	0	0	99	2.97	0	0	141	4.23	0	0	183	5.49	0	0
16	0.48	1	22.686	58	1.74	0	0	100	3	0	0	142	4.26	0	0	184	5.52	0	0
17	0.51	1	22.686	59	1.77	0	0	101	3.03	0	0	143	4.29	0	0	185	5.55	0	0
18	0.54	1	22.686	60	1.8	0	0	102	3.06	0	0	144	4.32	0	0	186	5.58	0	0
19	0.57	1	22.686	61	1.83	0	0	103	3.09	0	0	145	4.35	0	0	187	5.61	0	0
20	0.6	1	22.686	62	1.86	0	0	104	3.12	0	0	146	4.38	0	0	188	5.64	0	0
21	0.63	0.8	22.525	63	1.89	0	0	105	3.15	0	0	147	4.41	0	0	189	5.67	0	0
22	0.66	0.6	21.595	64	1.92	0	0	106	3.18	0	0	148	4.44	0	0	190	5.7	0	0
23	0.69	0.4	17.787	65	1.95	0	0	107	3.21	0	0	149	4.47	0	0	191	5.73	0	0
24	0.72	0.2	12.583	66	1.98	0	0	108	3.24	0	0	150	4.5	0	0	192	5.76	0	0
25	0.75	0	8.163	67	2.01	0	0	109	3.27	0	0	151	4.53	0	0	193	5.79	0	0
26	0.78	0	4.978	68	2.04	0	0	110	3.3	0	0	152	4.56	0	0	194	5.82	0	0
27	0.81	0	5.264	69	2.07	0	0	111	3.33	0	0	153	4.59	0	0	195	5.85	0	0
28	0.84	0	4.45	70	2.1	0	0	112	3.36	0	0	154	4.62	0	0	196	5.88	0	0
29	0.87	0	1.643	71	2.13	0	0	113	3.39	0	0	155	4.65	0	0	197	5.91	0	0
30	0.9	0	0.232	72	2.16	0	0	114	3.42	0	0	156	4.68	0	0	198	5.94	0	0
31	0.93	0	0.032	73	2.19	0	0	115	3.45	0	0	157	4.71	0	0	199	5.97	0	0
32	0.96	0	0	74	2.22	0	0	116	3.48	0	0	158	4.74	0	0	200	6	0	0
33	0.99	0	0	75	2.25	0	0	117	3.51	0	0	159	4.77	0	0				
34	1.02	0	0	76	2.28	0	0	118	3.54	0	0	160	4.8	0	0				
35	1.05	0	0	77	2.31	0	0	119	3.57	0	0	161	4.83	0	0				
36	1.08	0	0	78	2.34	0	0	120	3.6	0	0	162	4.86	0	0				
37	1.11	0	0	79	2.37	0	0	121	3.63	0	0	163	4.89	0	0				
38	1.14	0	0	80	2.4	0	0	122	3.66	0	0	164	4.92	0	0				
39	1.17	0	0	81	2.43	0	0	123	3.69	0	0	165	4.95	0	0				
40	1.2	0	0	82	2.46	0	0	124	3.72	0	0	166	4.98	0	0				
41	1.23	0	0	83	2.49	0	0	125	3.75	0	0	167	5.01	0	0				
42	1.26	0	0	84	2.52	0	0	126	3.78	0	0	168	5.04	0	0				

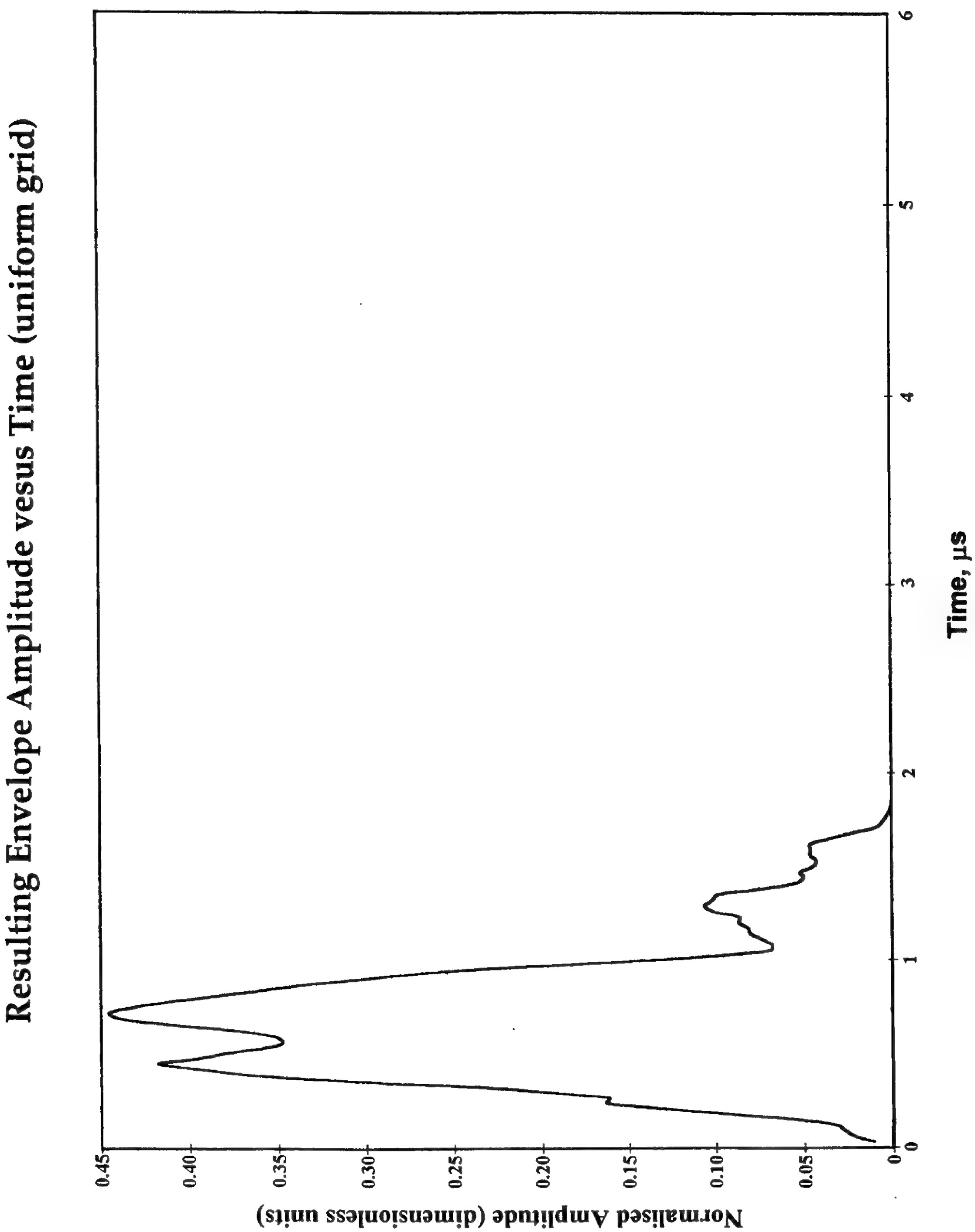
Resulting Envelope Amplitude vesus Time (uniform grid)
Normalised Amplitude (dimensionless units)
0.45
0.40
0.35
0.30
0.25
0.20
0.15
0.10
0.05
0
Time, µs
0
1
2
3
4
5
6

Beamwidth angle beta (degrees):	2
Great circle distance l (km):	300
Elevation angle phi (degrees):	5
Number of knots inside the scattering volume n:	1000
Operating frequency (MHz):	2800
Pulse rise time (μs):	0.1
Pulse width (μs):	0.5
Pulse fall time (μs):	0.15

i	Time[i]	Amplitude (arbitrary units)		i	Time[i]	Amplitude (arbitrary units)		i	Time[i]	Amplitude (arbitrary units)		i	Time[i]	Amplitude (arbitrary units)		i	Time[i]	Amplitude (arbitrary units)	
		Initial	Resulting			Initial	Resulting			Initial	Resulting			Initial	Resulting			Initial	Resulting
1	0.03	0.3	1.092	43	1.29	0	10.602	85	2.55	0	0	127	3.81	0	0	169	5.07	0	0
2	0.06	0.6	2.227	44	1.32	0	10.161	86	2.58	0	0	128	3.84	0	0	170	5.1	0	0
3	0.09	0.9	2.725	45	1.35	0	9.798	87	2.61	0	0	129	3.87	0	0	171	5.13	0	0
4	0.12	1	3.266	46	1.38	0	7.356	88	2.64	0	0	130	3.9	0	0	172	5.16	0	0
5	0.15	1	5.524	47	1.41	0	5.425	89	2.67	0	0	131	3.93	0	0	173	5.19	0	0
6	0.18	1	9.197	48	1.44	0	4.941	90	2.7	0	0	132	3.96	0	0	174	5.22	0	0
7	0.21	1	13.159	49	1.47	0	5.154	91	2.73	0	0	133	3.99	0	0	175	5.25	0	0
8	0.24	1	16.307	50	1.5	0	4.411	92	2.76	0	0	134	4.02	0	0	176	5.28	0	0
9	0.27	1	16.142	51	1.53	0	4.223	93	2.79	0	0	135	4.05	0	0	177	5.31	0	0
10	0.3	1	20.073	52	1.56	0	4.565	94	2.82	0	0	136	4.08	0	0	178	5.34	0	0
11	0.33	1	23.898	53	1.59	0	4.54	95	2.85	0	0	137	4.11	0	0	179	5.37	0	0
12	0.36	1	30.251	54	1.62	0	4.576	96	2.88	0	0	138	4.14	0	0	180	5.4	0	0
13	0.39	1	36.069	55	1.65	0	3.43	97	2.91	0	0	139	4.17	0	0	181	5.43	0	0
14	0.42	1	39.101	56	1.68	0	2.202	98	2.94	0	0	140	4.2	0	0	182	5.46	0	0
15	0.45	1	41.745	57	1.71	0	0.875	99	2.97	0	0	141	4.23	0	0	183	5.49	0	0
16	0.48	1	39.632	58	1.74	0	0.511	100	3	0	0	142	4.26	0	0	184	5.52	0	0
17	0.51	1	37.914	59	1.77	0	0.311	101	3.03	0	0	143	4.29	0	0	185	5.55	0	0
18	0.54	1	35.567	60	1.8	0	0.111	102	3.06	0	0	144	4.32	0	0	186	5.58	0	0
19	0.57	1	34.7	61	1.83	0	0	103	3.09	0	0	145	4.35	0	0	187	5.61	0	0
20	0.6	1	35.275	62	1.86	0	0	104	3.12	0	0	146	4.38	0	0	188	5.64	0	0
21	0.63	0.8	37.663	63	1.89	0	0	105	3.15	0	0	147	4.41	0	0	189	5.67	0	0
22	0.66	0.6	41.095	64	1.92	0	0	106	3.18	0	0	148	4.44	0	0	190	5.7	0	0
23	0.69	0.4	43.956	65	1.95	0	0	107	3.21	0	0	149	4.47	0	0	191	5.73	0	0
24	0.72	0.2	44.555	66	1.98	0	0	108	3.24	0	0	150	4.5	0	0	192	5.76	0	0
25	0.75	0	43.177	67	2.01	0	0	109	3.27	0	0	151	4.53	0	0	193	5.79	0	0
26	0.78	0	41.212	68	2.04	0	0	110	3.3	0	0	152	4.56	0	0	194	5.82	0	0
27	0.81	0	38.653	69	2.07	0	0	111	3.33	0	0	153	4.59	0	0	195	5.85	0	0
28	0.84	0	36.077	70	2.1	0	0	112	3.36	0	0	154	4.62	0	0	196	5.88	0	0
29	0.87	0	33.739	71	2.13	0	0	113	3.39	0	0	155	4.65	0	0	197	5.91	0	0
30	0.9	0	30.5	72	2.16	0	0	114	3.42	0	0	156	4.68	0	0	198	5.94	0	0
31	0.93	0	27.016	73	2.19	0	0	115	3.45	0	0	157	4.71	0	0	199	5.97	0	0
32	0.96	0	22.756	74	2.22	0	0	116	3.48	0	0	158	4.74	0	0	200	6	0	0
33	0.99	0	16.268	75	2.25	0	0	117	3.51	0	0	159	4.77	0	0				
34	1.02	0	10.254	76	2.28	0	0	118	3.54	0	0	160	4.8	0	0				
35	1.05	0	6.895	77	2.31	0	0	119	3.57	0	0	161	4.83	0	0				
36	1.08	0	6.736	78	2.34	0	0	120	3.6	0	0	162	4.86	0	0				
37	1.11	0	7.38	79	2.37	0	0	121	3.63	0	0	163	4.89	0	0				
38	1.14	0	7.985	80	2.4	0	0	122	3.66	0	0	164	4.92	0	0				
39	1.17	0	8.08	81	2.43	0	0	123	3.69	0	0	165	4.95	0	0				
40	1.2	0	8.666	82	2.46	0	0	124	3.72	0	0	166	4.98	0	0				
41	1.23	0	8.565	83	2.49	0	0	125	3.75	0	0	167	5.01	0	0				
42	1.26	0	10.117	84	2.52	0	0	126	3.78	0	0	168	5.04	0	0				

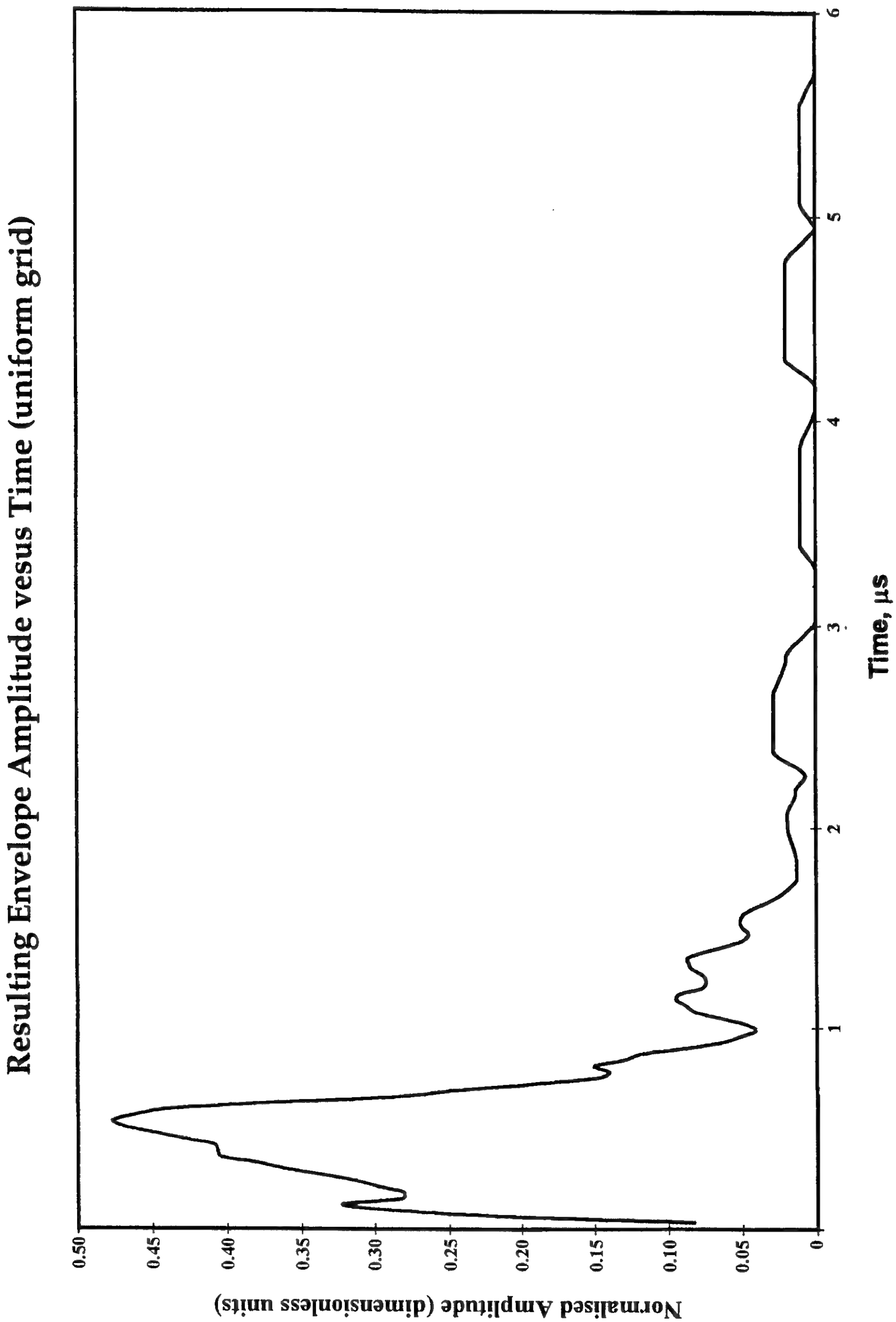
Resulting Envelope Amplitude vesus Time (uniform grid)
Normalised Amplitude (dimensionless units)
0.50
0.45
0.40
0.35
0.30
0.25
0.20
0.15
0.10
0.05
0
Time, µs
1
2
3
4
5
6

Beamwidth angle beta (degrees): 4
Great circle distance l (km): 300
Elevation angle phi (degrees): 2.1
Number of knots inside the scattering volume n: 1000
Operating frequency (MHz): 2830
Pulse rise time (μs): 0.1
Pulse width (μs): 0.5
Pulse fall time (μs): 0.15

i	Time[i]	Amplitude (arbitrary units)		i	Time[i]	Amplitude (arbitrary units)		i	Time[i]	Amplitude (arbitrary units)		i	Time[i]	Amplitude (arbitrary units)		i	Time[i]	Amplitude (arbitrary units)	
		Initial	Resulting			Initial	Resulting			Initial	Resulting			Initial	Resulting			Initial	Resulting
1	0.03	0.3	8.325	43	1.29	0	8.341	85	2.55	0	2.813	127	3.81	0	1	169	5.07	0	1
2	0.06	0.6	20.664	44	1.32	0	8.607	86	2.58	0	2.813	128	3.84	0	1	170	5.1	0	1
3	0.09	0.9	28.265	45	1.35	0	8.636	87	2.61	0	2.813	129	3.87	0	1	171	5.13	0	1
4	0.12	1	32.298	46	1.38	0	7.286	88	2.64	0	2.813	130	3.9	0	0.924	172	5.16	0	1
5	0.15	1	28.21	47	1.41	0	5.836	89	2.67	0	2.785	131	3.93	0	0.724	173	5.19	0	1
6	0.18	1	28.058	48	1.44	0	4.864	90	2.7	0	2.613	132	3.96	0	0.524	174	5.22	0	1
7	0.21	1	29.739	49	1.47	0	4.535	91	2.73	0	2.444	133	3.99	0	0.324	175	5.25	0	1
8	0.24	1	31.349	50	1.5	0	5.002	92	2.76	0	2.282	134	4.02	0	0.124	176	5.28	0	1
9	0.27	1	33.626	51	1.53	0	5.114	93	2.79	0	2.125	135	4.05	0	0	177	5.31	0	1
10	0.3	1	36.175	52	1.56	0	4.929	94	2.82	0	2	136	4.08	0	0	178	5.34	0	1
11	0.33	1	38.007	53	1.59	0	4.348	95	2.85	0	2	137	4.11	0	0	179	5.37	0	1
12	0.36	1	40.448	54	1.62	0	3.415	96	2.88	0	1.749	138	4.14	0	0	180	5.4	0	1
13	0.39	1	40.695	55	1.65	0	2.604	97	2.91	0	1.349	139	4.17	0	0	181	5.43	0	1
14	0.42	1	40.907	56	1.68	0	2.063	98	2.94	0	0.949	140	4.2	0	0.319	182	5.46	0	1
15	0.45	1	43.108	57	1.71	0	1.641	99	2.97	0	0.549	141	4.23	0	0.919	183	5.49	0	1
16	0.48	1	44.858	58	1.74	0	1.285	100	3	0	0.149	142	4.26	0	1.519	184	5.52	0	1
17	0.51	1	46.885	59	1.77	0	1.285	101	3.03	0	0	143	4.29	0	2	185	5.55	0	1
18	0.54	1	47.681	60	1.8	0	1.285	102	3.06	0	0	144	4.32	0	2	186	5.58	0	0.816
19	0.57	1	46.215	61	1.83	0	1.285	103	3.09	0	0	145	4.35	0	2	187	5.61	0	0.616
20	0.6	1	43.815	62	1.86	0	1.361	104	3.12	0	0	146	4.38	0	2	188	5.64	0	0.416
21	0.63	0.8	37.396	63	1.89	0	1.47	105	3.15	0	0	147	4.41	0	2	189	5.67	0	0.216
22	0.66	0.6	28.39	64	1.92	0	1.597	106	3.18	0	0	148	4.44	0	2	190	5.7	0	0.016
23	0.69	0.4	24.574	65	1.95	0	1.731	107	3.21	0	0	149	4.47	0	2	191	5.73	0	0
24	0.72	0.2	19.463	66	1.98	0	1.864	108	3.24	0	0	150	4.5	0	2	192	5.76	0	0
25	0.75	0	14.717	67	2.01	0	1.893	109	3.27	0	0	151	4.53	0	2	193	5.79	0	0
26	0.78	0	13.98	68	2.04	0	1.922	110	3.3	0	0.114	152	4.56	0	2	194	5.82	0	0
27	0.81	0	14.974	69	2.07	0	1.934	111	3.33	0	0.414	153	4.59	0	2	195	5.85	0	0
28	0.84	0	12.969	70	2.1	0	1.73	112	3.36	0	0.714	154	4.62	0	2	196	5.88	0	0
29	0.87	0	11.699	71	2.13	0	1.524	113	3.39	0	1	155	4.65	0	2	197	5.91	0	0
30	0.9	0	8.735	72	2.16	0	1.354	114	3.42	0	1	156	4.68	0	2	198	5.94	0	0
31	0.93	0	6.322	73	2.19	0	1.322	115	3.45	0	1	157	4.71	0	2	199	5.97	0	0
32	0.96	0	5.021	74	2.22	0	0.98	116	3.48	0	1	158	4.74	0	2	200	6	0	0
33	0.99	0	4.079	75	2.25	0	0.703	117	3.51	0	1	159	4.77	0	2				
34	1.02	0	4.917	76	2.28	0	0.963	118	3.54	0	1	160	4.8	0	1.788				
35	1.05	0	6.483	77	2.31	0	1.86	119	3.57	0	1	161	4.83	0	1.388				
36	1.08	0	8.225	78	2.34	0	2.405	120	3.6	0	1	162	4.86	0	0.988				
37	1.11	0	8.815	79	2.37	0	2.813	121	3.63	0	1	163	4.89	0	0.588				
38	1.14	0	9.458	80	2.4	0	2.813	122	3.66	0	1	164	4.92	0	0.188				
39	1.17	0	9.176	81	2.43	0	2.813	123	3.69	0	1	165	4.95	0	0				
40	1.2	0	7.649	82	2.46	0	2.813	124	3.72	0	1	166	4.98	0	0.276				
41	1.23	0	7.412	83	2.49	0	2.813	125	3.75	0	1	167	5.01	0	0.576				
42	1.26	0	7.625	84	2.52	0	2.813	126	3.78	0	1	168	5.04	0	0.876				

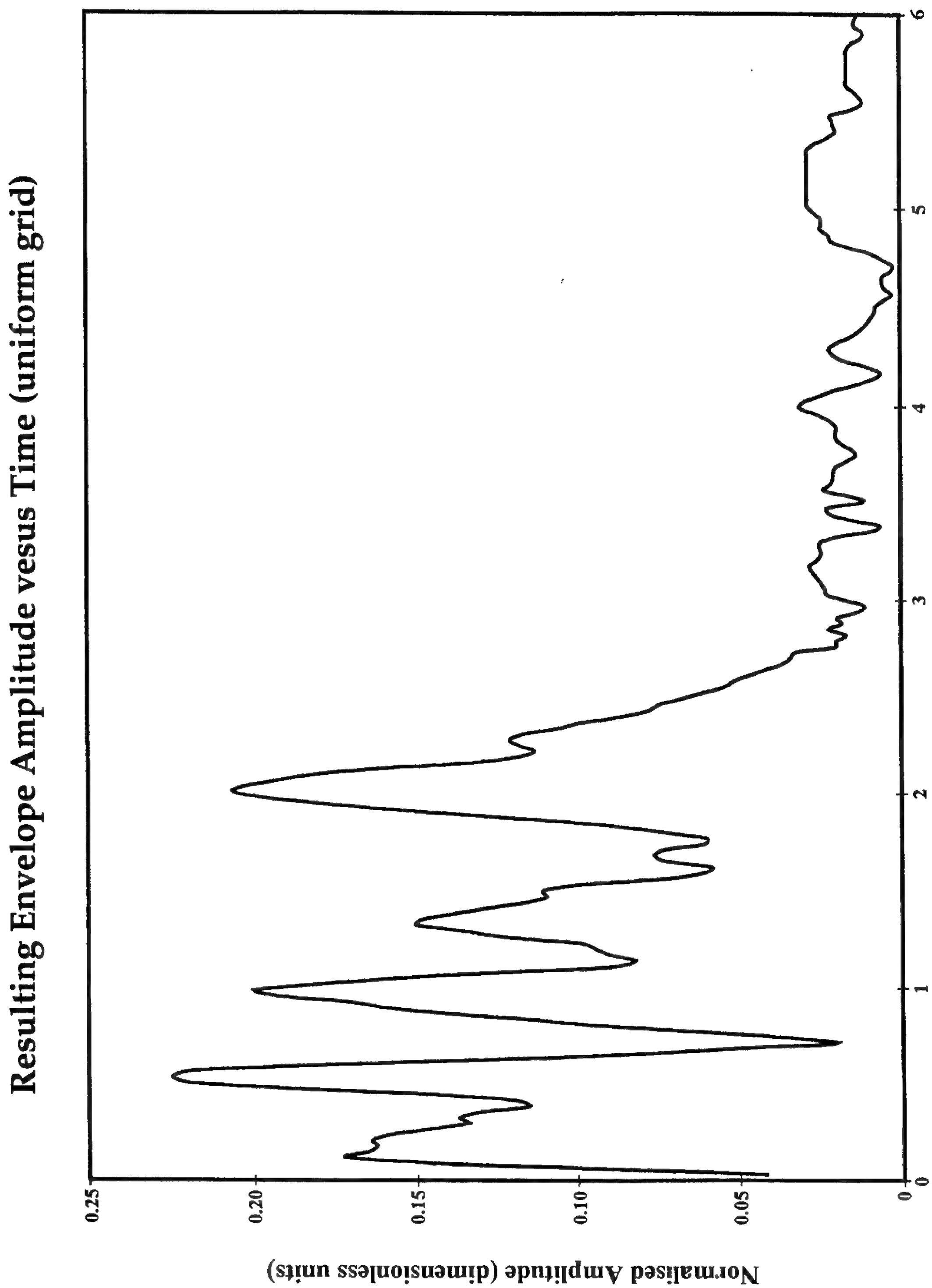
Resulting Envelope Amplitude vesus Time (uniform grid)
Normalised Amplitude (dimensionless units)
0.25
0.20
0.15
0.10
0.05
0
0
1
2
3
4
5
6
Time, µs

Beamwidth angle beta (degrees):	8
Great circle distance l (km):	300
Elevation angle phi (degrees):	4.1
Number of knots inside the scattering volume n:	1000
Operating frequency (MHz):	2830
Pulse rise time (μs):	0.1
Pulse width (μs):	0.5
Pulse fall time (μs):	0.15

i	Time[i]	Amplitude (arbitrary units)		i	Time[i]	Amplitude (arbitrary units)		i	Time[i]	Amplitude (arbitrary units)		i	Time[i]	Amplitude (arbitrary units)		i	Time[i]	Amplitude (arbitrary units)	
		Initial	Resulting			Initial	Resulting			Initial	Resulting			Initial	Resulting			Initial	Resulting
1	0.03	0.3	4.2	43	1.29	0	13.484	85	2.55	0	5.451	127	3.81	0	1.793	169	5.07	0	2.836
2	0.06	0.6	9.2	44	1.32	0	15	86	2.58	0	5.115	128	3.84	0	1.981	170	5.1	0	2.836
3	0.09	0.9	14.26	45	1.35	0	14.854	87	2.61	0	4.66	129	3.87	0	1.981	171	5.13	0	2.836
4	0.12	1	17.176	46	1.38	0	13.859	88	2.64	0	4.168	130	3.9	0	1.981	172	5.16	0	2.836
5	0.15	1	16.486	47	1.41	0	12.773	89	2.67	0	3.634	131	3.93	0	2.186	173	5.19	0	2.836
6	0.18	1	16.243	48	1.44	0	11.524	90	2.7	0	3.373	132	3.96	0	2.555	174	5.22	0	2.836
7	0.21	1	16.386	49	1.47	0	10.928	91	2.73	0	3.22	133	3.99	0	3.061	175	5.25	0	2.836
8	0.24	1	15.854	50	1.5	0	11.034	92	2.76	0	2.017	134	4.02	0	2.968	176	5.28	0	2.836
9	0.27	1	14.569	51	1.53	0	9.837	93	2.79	0	1.989	135	4.05	0	2.538	177	5.31	0	2.836
10	0.3	1	13.437	52	1.56	0	7.151	94	2.82	0	1.685	136	4.08	0	2.041	178	5.34	0	2.635
11	0.33	1	13.681	53	1.59	0	8.056	95	2.85	0	2.208	137	4.11	0	1.336	179	5.37	0	2.249
12	0.36	1	13.045	54	1.62	0	5.626	96	2.88	0	1.81	138	4.14	0	0.77	180	5.4	0	1.98
13	0.39	1	11.505	55	1.65	0	7.212	97	2.91	0	1.938	139	4.17	0	0.612	181	5.43	0	2.017
14	0.42	1	11.937	56	1.68	0	7.585	98	2.94	0	1.316	140	4.2	0	1.077	182	5.46	0	2.064
15	0.45	1	14.357	57	1.71	0	7.246	99	2.97	0	1.122	141	4.23	0	1.803	183	5.49	0	2.1
16	0.48	1	18.554	58	1.74	0	6.036	100	3	0	1.761	142	4.26	0	2.102	184	5.52	0	1.45
17	0.51	1	21.987	59	1.77	0	5.97	101	3.03	0	2.265	143	4.29	0	2.176	185	5.55	0	1.144
18	0.54	1	22.489	60	1.8	0	7.327	102	3.06	0	2.339	144	4.32	0	1.903	186	5.58	0	1.233
19	0.57	1	21.963	61	1.83	0	8.785	103	3.09	0	2.446	145	4.35	0	1.478	187	5.61	0	1.424
20	0.6	1	18.666	62	1.86	0	10.634	104	3.12	0	2.603	146	4.38	0	1.22	188	5.64	0	1.638
21	0.63	0.8	13.431	63	1.89	0	13.298	105	3.15	0	2.713	147	4.41	0	1.039	189	5.67	0	1.638
22	0.66	0.6	8.402	64	1.92	0	16.002	106	3.18	0	2.791	148	4.44	0	0.902	190	5.7	0	1.638
23	0.69	0.4	5.118	65	1.95	0	18.004	107	3.21	0	2.539	149	4.47	0	0.788	191	5.73	0	1.638
24	0.72	0.2	2.062	66	1.98	0	19.544	108	3.24	0	2.427	150	4.5	0	0.727	192	5.76	0	1.638
25	0.75	0	3.752	67	2.01	0	20.59	109	3.27	0	2.491	151	4.53	0	0.478	193	5.79	0	1.638
26	0.78	0	6.348	68	2.04	0	20.262	110	3.3	0	2.463	152	4.56	0	0.274	194	5.82	0	1.638
27	0.81	0	9.377	69	2.07	0	19.236	111	3.33	0	1.987	153	4.59	0	0.491	195	5.85	0	1.494
28	0.84	0	11.257	70	2.1	0	18.03	112	3.36	0	0.858	154	4.62	0	0.55	196	5.88	0	1.185
29	0.87	0	13.937	71	2.13	0	16.221	113	3.39	0	0.643	155	4.65	0	0.537	197	5.91	0	1.139
30	0.9	0	15.914	72	2.16	0	13.427	114	3.42	0	1.614	156	4.68	0	0.28	198	5.94	0	1.379
31	0.93	0	17.166	73	2.19	0	11.844	115	3.45	0	2.226	157	4.71	0	0.236	199	5.97	0	1.379
32	0.96	0	19.168	74	2.22	0	11.283	116	3.48	0	2.219	158	4.74	0	0.582	200	6	0	1.289
33	0.99	0	19.947	75	2.25	0	11.751	117	3.51	0	1.153	159	4.77	0	0.935				
34	1.02	0	18.085	76	2.28	0	12.079	118	3.54	0	1.536	160	4.8	0	1.556				
35	1.05	0	15.624	77	2.31	0	11.653	119	3.57	0	2.346	161	4.83	0	2.096				
36	1.08	0	12.471	78	2.34	0	10.515	120	3.6	0	2.156	162	4.86	0	2.189				
37	1.11	0	9.01	79	2.37	0	9.894	121	3.63	0	2.068	163	4.89	0	2.427				
38	1.14	0	8.165	80	2.4	0	8.612	122	3.66	0	2.07	164	4.92	0	2.426				
39	1.17	0	8.997	81	2.43	0	7.762	123	3.69	0	1.996	165	4.95	0	2.436				
40	1.2	0	9.42	82	2.46	0	7.415	124	3.72	0	1.679	166	4.98	0	2.629				
41	1.23	0	9.895	83	2.49	0	6.776	125	3.75	0	1.385	167	5.01	0	2.824				
42	1.26	0	12.134	84	2.52	0	6.125	126	3.78	0	1.481	168	5.04	0	2.836				

Appendix B: Computations of Radar Pulse Envelope Distortion for Random Distribution

Grid with random distribution of knots

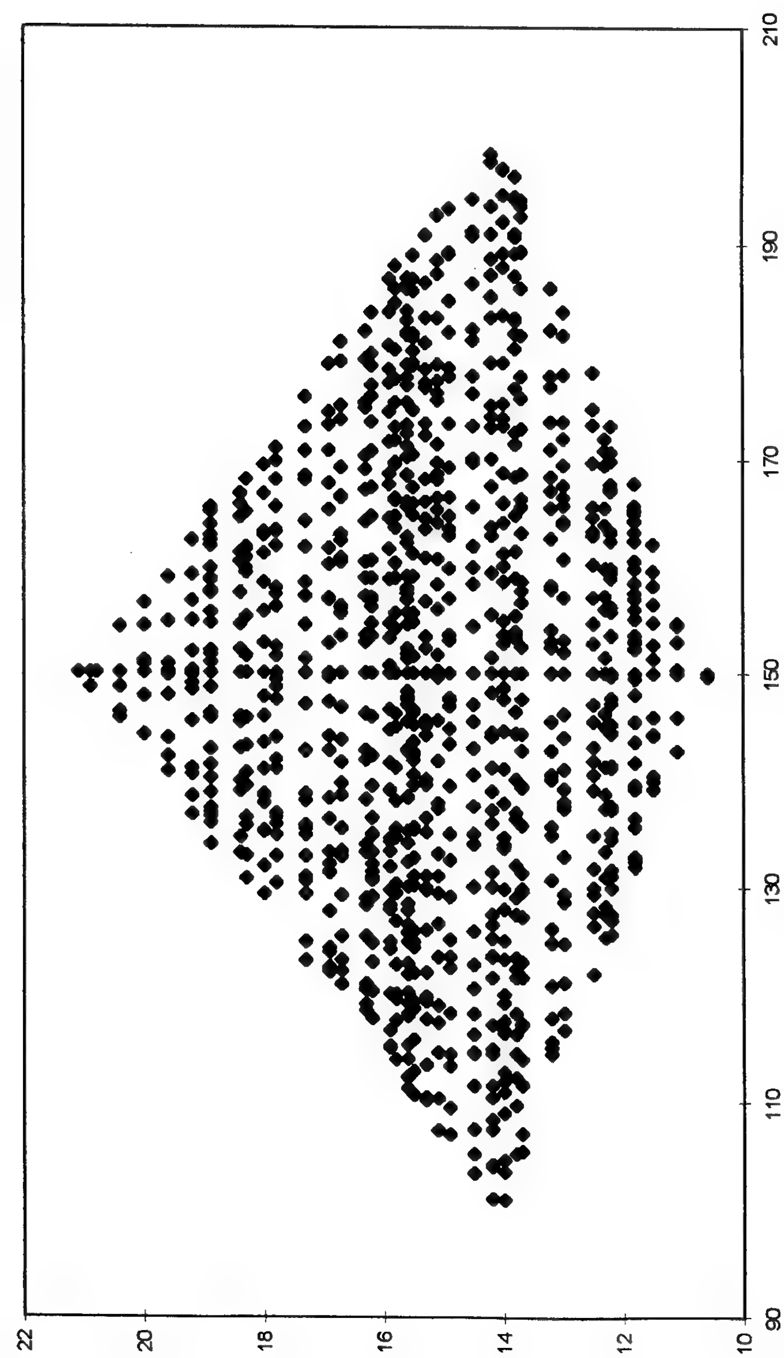

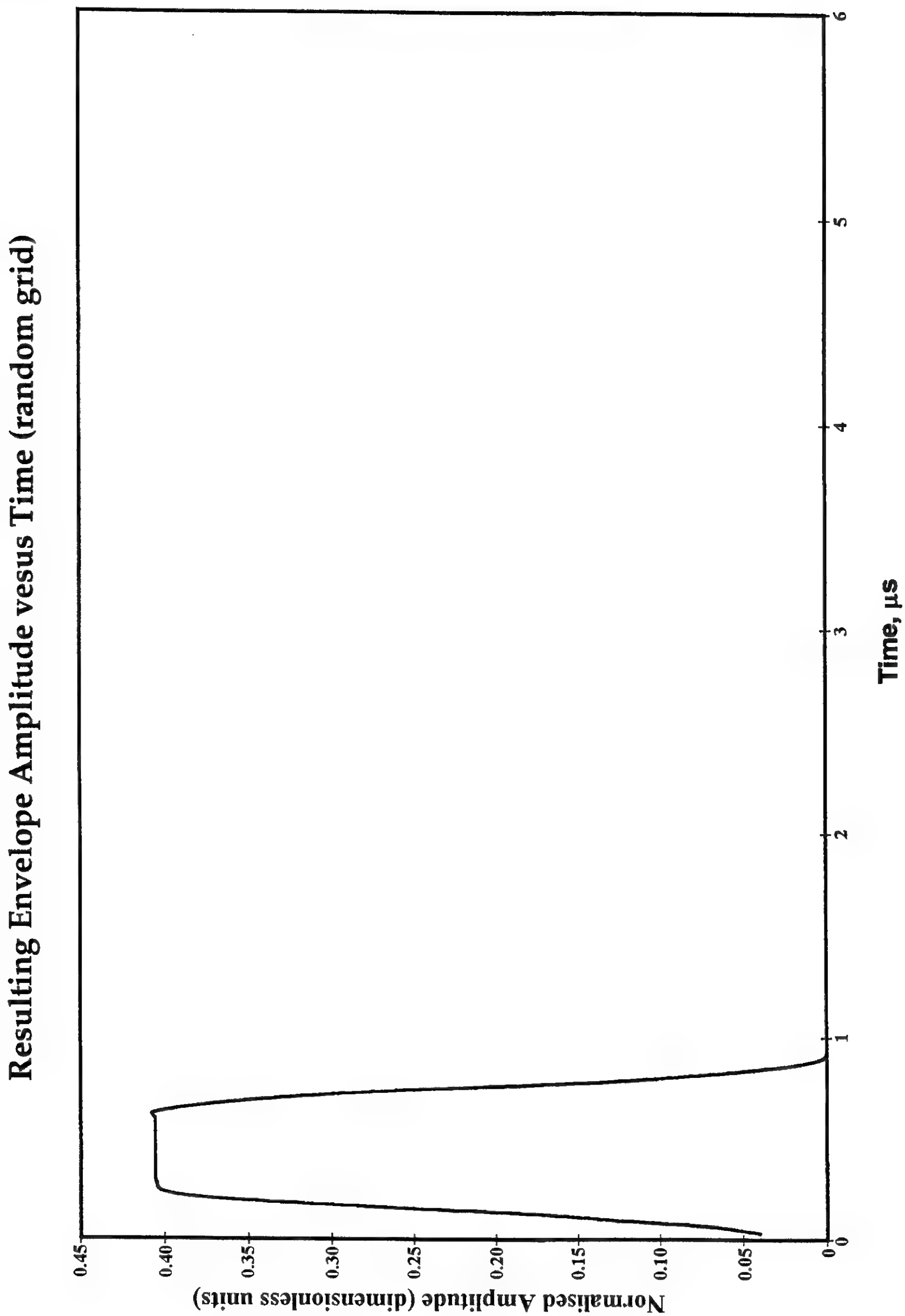
Resulting Envelope Amplitude vesus Time (random grid)
Normalised Amplitude (dimensionless units)
0.45
0.40
0.35
0.30
0.25
0.20
0.15
0.10
0.05
0
Time, µs
0
1
2
3
4
5
6

Beamwidth angle beta (degrees): 1.2
Great circle distance l (km): 300
Elevation angle phi (degrees): 0.7
Number of knots inside the scattering volume n: 1000
Operating frequency (MHz): 2830
Pulse rise time (μs): 0.1
Pulse width (μs): 0.5
Pulse fall time (μs): 0.15

i	Time[i]	Amplitude (arbitrary units)		i	Time[i]	Amplitude (arbitrary units)		i	Time[i]	Amplitude (arbitrary units)		i	Time[i]	Amplitude (arbitrary units)		i	Time[i]	Amplitude (arbitrary units)	
		Initial	Resulting			Initial	Resulting			Initial	Resulting			Initial	Resulting			Initial	Resulting
1	0.03	0.3	4.012	43	1.29	0	0	85	2.55	0	0	127	3.81	0	0	169	5.07	0	0
2	0.06	0.6	7.129	44	1.32	0	0	86	2.58	0	0	128	3.84	0	0	170	5.1	0	0
3	0.09	0.9	12.174	45	1.35	0	0	87	2.61	0	0	129	3.87	0	0	171	5.13	0	0
4	0.12	1	17.2	46	1.38	0	0	88	2.64	0	0	130	3.9	0	0	172	5.16	0	0
5	0.15	1	25.452	47	1.41	0	0	89	2.67	0	0	131	3.93	0	0	173	5.19	0	0
6	0.18	1	33.082	48	1.44	0	0	90	2.7	0	0	132	3.96	0	0	174	5.22	0	0
7	0.21	1	38.284	49	1.47	0	0	91	2.73	0	0	133	3.99	0	0	175	5.25	0	0
8	0.24	1	40.247	50	1.5	0	0	92	2.76	0	0	134	4.02	0	0	176	5.28	0	0
9	0.27	1	40.471	51	1.53	0	0	93	2.79	0	0	135	4.05	0	0	177	5.31	0	0
10	0.3	1	40.558	52	1.56	0	0	94	2.82	0	0	136	4.08	0	0	178	5.34	0	0
11	0.33	1	40.558	53	1.59	0	0	95	2.85	0	0	137	4.11	0	0	179	5.37	0	0
12	0.36	1	40.558	54	1.62	0	0	96	2.88	0	0	138	4.14	0	0	180	5.4	0	0
13	0.39	1	40.558	55	1.65	0	0	97	2.91	0	0	139	4.17	0	0	181	5.43	0	0
14	0.42	1	40.558	56	1.68	0	0	98	2.94	0	0	140	4.2	0	0	182	5.46	0	0
15	0.45	1	40.558	57	1.71	0	0	99	2.97	0	0	141	4.23	0	0	183	5.49	0	0
16	0.48	1	40.558	58	1.74	0	0	100	3	0	0	142	4.26	0	0	184	5.52	0	0
17	0.51	1	40.558	59	1.77	0	0	101	3.03	0	0	143	4.29	0	0	185	5.55	0	0
18	0.54	1	40.558	60	1.8	0	0	102	3.06	0	0	144	4.32	0	0	186	5.58	0	0
19	0.57	1	40.558	61	1.83	0	0	103	3.09	0	0	145	4.35	0	0	187	5.61	0	0
20	0.6	1	40.558	62	1.86	0	0	104	3.12	0	0	146	4.38	0	0	188	5.64	0	0
21	0.63	0.8	40.731	63	1.89	0	0	105	3.15	0	0	147	4.41	0	0	189	5.67	0	0
22	0.66	0.6	38.705	64	1.92	0	0	106	3.18	0	0	148	4.44	0	0	190	5.7	0	0
23	0.69	0.4	35.273	65	1.95	0	0	107	3.21	0	0	149	4.47	0	0	191	5.73	0	0
24	0.72	0.2	30.394	66	1.98	0	0	108	3.24	0	0	150	4.5	0	0	192	5.76	0	0
25	0.75	0	22.659	67	2.01	0	0	109	3.27	0	0	151	4.53	0	0	193	5.79	0	0
26	0.78	0	14.311	68	2.04	0	0	110	3.3	0	0	152	4.56	0	0	194	5.82	0	0
27	0.81	0	8.296	69	2.07	0	0	111	3.33	0	0	153	4.59	0	0	195	5.85	0	0
28	0.84	0	4.151	70	2.1	0	0	112	3.36	0	0	154	4.62	0	0	196	5.88	0	0
29	0.87	0	1.484	71	2.13	0	0	113	3.39	0	0	155	4.65	0	0	197	5.91	0	0
30	0.9	0	0.2	72	2.16	0	0	114	3.42	0	0	156	4.68	0	0	198	5.94	0	0
31	0.93	0	0	73	2.19	0	0	115	3.45	0	0	157	4.71	0	0	199	5.97	0	0
32	0.96	0	0	74	2.22	0	0	116	3.48	0	0	158	4.74	0	0	200	6	0	0
33	0.99	0	0	75	2.25	0	0	117	3.51	0	0	159	4.77	0	0				
34	1.02	0	0	76	2.28	0	0	118	3.54	0	0	160	4.8	0	0				
35	1.05	0	0	77	2.31	0	0	119	3.57	0	0	161	4.83	0	0				
36	1.08	0	0	78	2.34	0	0	120	3.6	0	0	162	4.86	0	0				
37	1.11	0	0	79	2.37	0	0	121	3.63	0	0	163	4.89	0	0				
38	1.14	0	0	80	2.4	0	0	122	3.66	0	0	164	4.92	0	0				
39	1.17	0	0	81	2.43	0	0	123	3.69	0	0	165	4.95	0	0				
40	1.2	0	0	82	2.46	0	0	124	3.72	0	0	166	4.98	0	0				
41	1.23	0	0	83	2.49	0	0	125	3.75	0	0	167	5.01	0	0				
42	1.26	0	0	84	2.52	0	0	126	3.78	0	0	168	5.04	0	0				

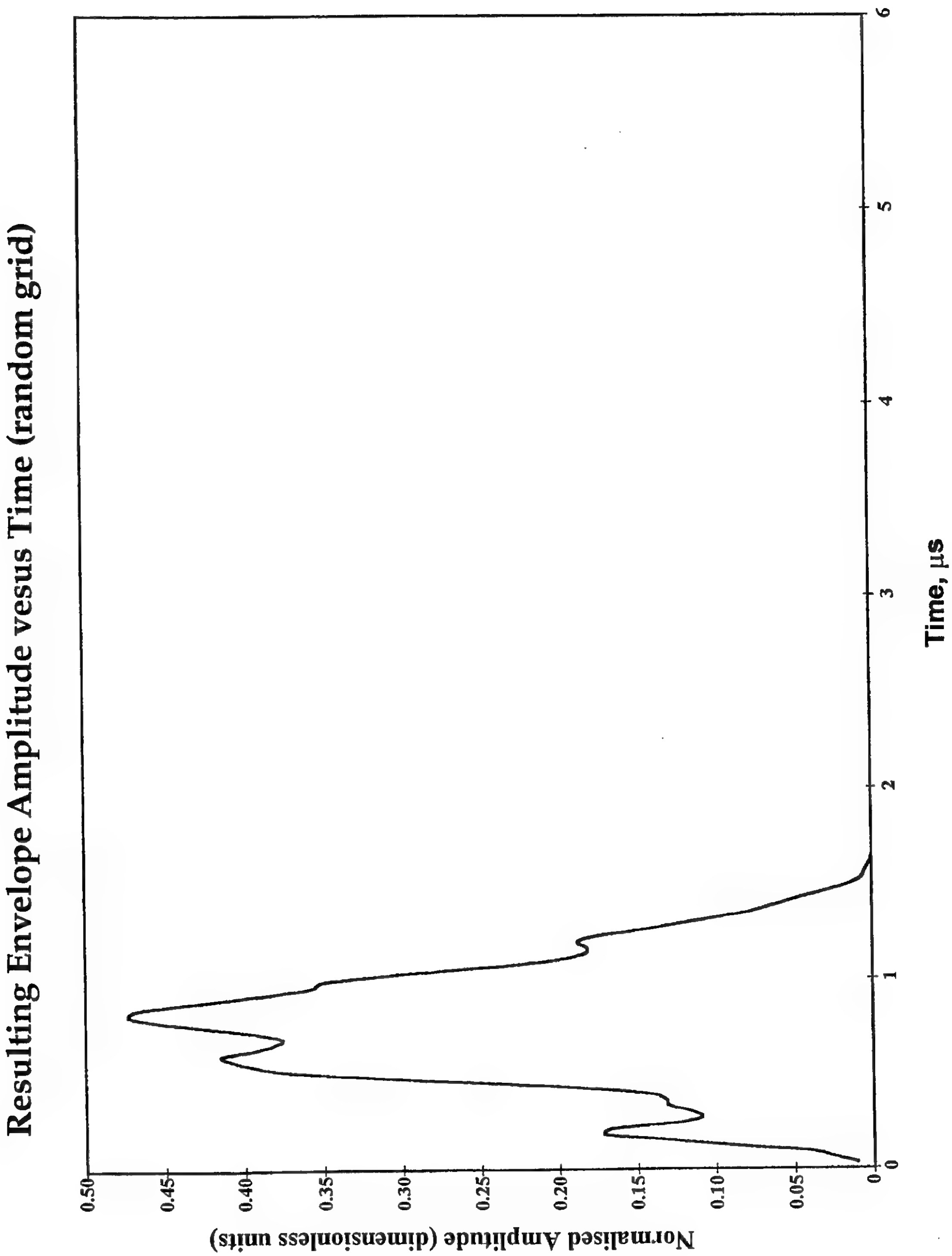

Resulting Envelope Amplitude vesus Time (random grid)
Normalised Amplitude (dimensionless units)
0.50
0.45
0.40
0.35
0.30
0.25
0.20
0.15
0.10
0.05
0
Time, µs
0
1
2
3
4
5
6

Beamwidth angle beta (degrees):	2
Great circle distance l (km):	300
Elevation angle phi (degrees):	4
Number of knots inside the scattering volume n:	1000
Operating frequency (MHz):	2800
Pulse rise time (μs):	0.1
Pulse width (μs):	0.5
Pulse fall time (μs):	0.15

i	Time[i]	Amplitude (arbitrary units)		i	Time[i]	Amplitude (arbitrary units)		i	Time[i]	Amplitude (arbitrary units)		i	Time[i]	Amplitude (arbitrary units)		i	Time[i]	Amplitude (arbitrary units)	
		Initial	Resulting			Initial	Resulting			Initial	Resulting			Initial	Resulting			Initial	Resulting
1	0.03	0.3	1.055	43	1.29	0	12.628	85	2.55	0	0	127	3.81	0	0	169	5.07	0	0
2	0.06	0.6	2.412	44	1.32	0	10.248	86	2.58	0	0	128	3.84	0	0	170	5.1	0	0
3	0.09	0.9	4.094	45	1.35	0	7.891	87	2.61	0	0	129	3.87	0	0	171	5.13	0	0
4	0.12	1	8.946	46	1.38	0	6.667	88	2.64	0	0	130	3.9	0	0	172	5.16	0	0
5	0.15	1	13.161	47	1.41	0	5.317	89	2.67	0	0	131	3.93	0	0	173	5.19	0	0
6	0.18	1	17.091	48	1.44	0	3.978	90	2.7	0	0	132	3.96	0	0	174	5.22	0	0
7	0.21	1	16.751	49	1.47	0	2.668	91	2.73	0	0	133	3.99	0	0	175	5.25	0	0
8	0.24	1	12.496	50	1.5	0	1.374	92	2.76	0	0	134	4.02	0	0	176	5.28	0	0
9	0.27	1	10.864	51	1.53	0	0.693	93	2.79	0	0	135	4.05	0	0	177	5.31	0	0
10	0.3	1	11.494	52	1.56	0	0.493	94	2.82	0	0	136	4.08	0	0	178	5.34	0	0
11	0.33	1	13.042	53	1.59	0	0.293	95	2.85	0	0	137	4.11	0	0	179	5.37	0	0
12	0.36	1	13.158	54	1.62	0	0.093	96	2.88	0	0	138	4.14	0	0	180	5.4	0	0
13	0.39	1	13.967	55	1.65	0	0	97	2.91	0	0	139	4.17	0	0	181	5.43	0	0
14	0.42	1	17.627	56	1.68	0	0	98	2.94	0	0	140	4.2	0	0	182	5.46	0	0
15	0.45	1	24.203	57	1.71	0	0	99	2.97	0	0	141	4.23	0	0	183	5.49	0	0
16	0.48	1	30.908	58	1.74	0	0	100	3	0	0	142	4.26	0	0	184	5.52	0	0
17	0.51	1	36.937	59	1.77	0	0	101	3.03	0	0	143	4.29	0	0	185	5.55	0	0
18	0.54	1	39.337	60	1.8	0	0	102	3.06	0	0	144	4.32	0	0	186	5.58	0	0
19	0.57	1	40.692	61	1.83	0	0	103	3.09	0	0	145	4.35	0	0	187	5.61	0	0
20	0.6	1	41.491	62	1.86	0	0	104	3.12	0	0	146	4.38	0	0	188	5.64	0	0
21	0.63	0.8	39.367	63	1.89	0	0	105	3.15	0	0	147	4.41	0	0	189	5.67	0	0
22	0.66	0.6	38.169	64	1.92	0	0	106	3.18	0	0	148	4.44	0	0	190	5.7	0	0
23	0.69	0.4	37.601	65	1.95	0	0	107	3.21	0	0	149	4.47	0	0	191	5.73	0	0
24	0.72	0.2	39.528	66	1.98	0	0	108	3.24	0	0	150	4.5	0	0	192	5.76	0	0
25	0.75	0	42.72	67	2.01	0	0	109	3.27	0	0	151	4.53	0	0	193	5.79	0	0
26	0.78	0	45.483	68	2.04	0	0	110	3.3	0	0	152	4.56	0	0	194	5.82	0	0
27	0.81	0	47.33	69	2.07	0	0	111	3.33	0	0	153	4.59	0	0	195	5.85	0	0
28	0.84	0	46.909	70	2.1	0	0	112	3.36	0	0	154	4.62	0	0	196	5.88	0	0
29	0.87	0	44.501	71	2.13	0	0	113	3.39	0	0	155	4.65	0	0	197	5.91	0	0
30	0.9	0	41.046	72	2.16	0	0	114	3.42	0	0	156	4.68	0	0	198	5.94	0	0
31	0.93	0	37.939	73	2.19	0	0	115	3.45	0	0	157	4.71	0	0	199	5.97	0	0
32	0.96	0	35.688	74	2.22	0	0	116	3.48	0	0	158	4.74	0	0	200	6	0	0
33	0.99	0	35.073	75	2.25	0	0	117	3.51	0	0	159	4.77	0	0				
34	1.02	0	31.582	76	2.28	0	0	118	3.54	0	0	160	4.8	0	0				
35	1.05	0	26.922	77	2.31	0	0	119	3.57	0	0	161	4.83	0	0				
36	1.08	0	22.673	78	2.34	0	0	120	3.6	0	0	162	4.86	0	0				
37	1.11	0	19.573	79	2.37	0	0	121	3.63	0	0	163	4.89	0	0				
38	1.14	0	18.176	80	2.4	0	0	122	3.66	0	0	164	4.92	0	0				
39	1.17	0	18.173	81	2.43	0	0	123	3.69	0	0	165	4.95	0	0				
40	1.2	0	18.727	82	2.46	0	0	124	3.72	0	0	166	4.98	0	0				
41	1.23	0	17.545	83	2.49	0	0	125	3.75	0	0	167	5.01	0	0				
42	1.26	0	15.012	84	2.52	0	0	126	3.78	0	0	168	5.04	0	0				

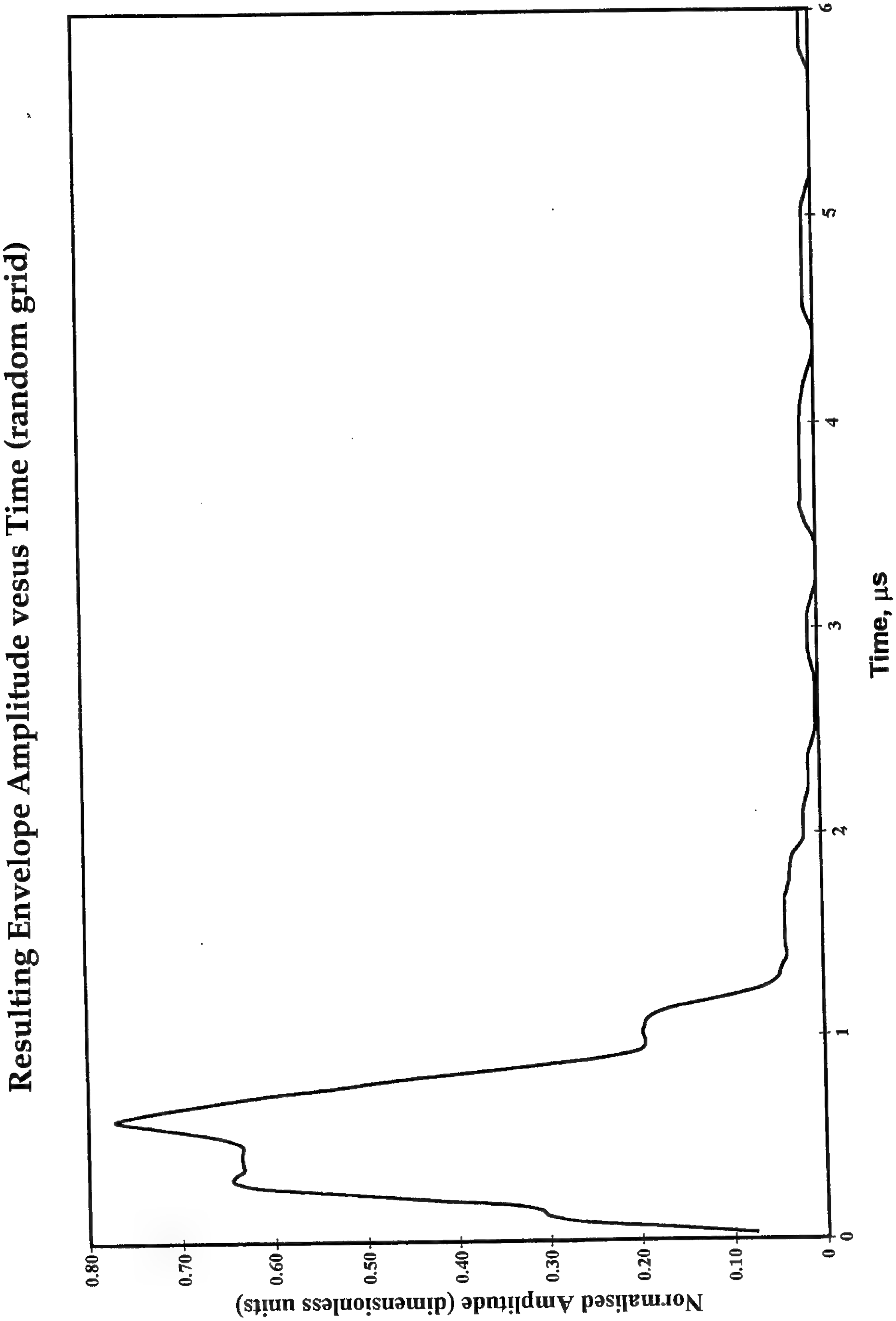
Resulting Envelope Amplitude vesus Time (random grid)
Normalised Amplitude (dimensionless units)
0.80
0.70
0.60
0.50
0.40
0.30
0.20
0.10
0
Time, μs
0
1
2
3
4
5
6

Beamwidth angle beta (degrees):	4
Great circle distance l (km):	300
Elevation angle phi (degrees):	2.1
Number of knots inside the scattering volume n:	1000
Operating frequency (MHz):	2830
Pulse rise time (μs):	0.1
Pulse width (μs):	0.5
Pulse fall time (μs):	0.15

i	Time[i]	Amplitude (arbitrary units)		i	Time[i]	Amplitude (arbitrary units)		i	Time[i]	Amplitude (arbitrary units)		i	Time[i]	Amplitude (arbitrary units)		i	Time[i]	Amplitude (arbitrary units)	
		Initial	Resulting			Initial	Resulting			Initial	Resulting			Initial	Resulting			Initial	Resulting
1	0.03	0.3	7.796	43	1.29	0	4.73	85	2.55	0	0.349	127	3.81	0	1.573	169	5.07	0	0.832
2	0.06	0.6	16.812	44	1.32	0	4.598	86	2.58	0	0.347	128	3.84	0	1.573	170	5.1	0	0.632
3	0.09	0.9	26.132	45	1.35	0	4.287	87	2.61	0	0.347	129	3.87	0	1.573	171	5.13	0	0.432
4	0.12	1	30.115	46	1.38	0	3.913	88	2.64	0	0.347	130	3.9	0	1.573	172	5.16	0	0.232
5	0.15	1	31.009	47	1.41	0	3.91	89	2.67	0	0.347	131	3.93	0	1.573	173	5.19	0	0.032
6	0.18	1	35.371	48	1.44	0	3.998	90	2.7	0	0.347	132	3.96	0	1.573	174	5.22	0	0
7	0.21	1	44.845	49	1.47	0	3.998	91	2.73	0	0.343	133	3.99	0	1.573	175	5.25	0	0
8	0.24	1	53.907	50	1.5	0	3.998	92	2.76	0	0.414	134	4.02	0	1.547	176	5.28	0	0
9	0.27	1	61.915	51	1.53	0	3.998	93	2.79	0	0.552	135	4.05	0	1.477	177	5.31	0	0
10	0.3	1	64.519	52	1.56	0	3.998	94	2.82	0	0.72	136	4.08	0	1.432	178	5.34	0	0
11	0.33	1	64.268	53	1.59	0	3.998	95	2.85	0	0.901	137	4.11	0	1.337	179	5.37	0	0
12	0.36	1	63.382	54	1.62	0	3.998	96	2.88	0	1	138	4.14	0	1.21	180	5.4	0	0
13	0.39	1	63.526	55	1.65	0	3.998	97	2.91	0	1	139	4.17	0	1.144	181	5.43	0	0
14	0.42	1	63.575	56	1.68	0	3.998	98	2.94	0	1	140	4.2	0	0.954	182	5.46	0	0
15	0.45	1	63.529	57	1.71	0	3.828	99	2.97	0	1	141	4.23	0	0.701	183	5.49	0	0
16	0.48	1	63.522	58	1.74	0	3.619	100	3	0	1	142	4.26	0	0.487	184	5.52	0	0
17	0.51	1	65.248	59	1.77	0	3.449	101	3.03	0	1	143	4.29	0	0.287	185	5.55	0	0
18	0.54	1	68.462	60	1.8	0	3.491	102	3.06	0	1	144	4.32	0	0.087	186	5.58	0	0
19	0.57	1	73.087	61	1.83	0	3.374	103	3.09	0	0.891	145	4.35	0	0	187	5.61	0	0
20	0.6	1	77.048	62	1.86	0	3.279	104	3.12	0	0.691	146	4.38	0	0	188	5.64	0	0
21	0.63	0.8	75.013	63	1.89	0	3.062	105	3.15	0	0.491	147	4.41	0	0	189	5.67	0	0
22	0.66	0.6	70.84	64	1.92	0	2.574	106	3.18	0	0.291	148	4.44	0	0	190	5.7	0	0
23	0.69	0.4	66.171	65	1.95	0	2.047	107	3.21	0	0.091	149	4.47	0	0.253	191	5.73	0	0.254
24	0.72	0.2	61.137	66	1.98	0	1.855	108	3.24	0	0	150	4.5	0	0.553	192	5.76	0	0.554
25	0.75	0	54.312	67	2.01	0	1.855	109	3.27	0	0	151	4.53	0	0.853	193	5.79	0	0.854
26	0.78	0	49.432	68	2.04	0	1.855	110	3.3	0	0	152	4.56	0	1	194	5.82	0	1
27	0.81	0	43.191	69	2.07	0	1.855	111	3.33	0	0	153	4.59	0	1	195	5.85	0	1
28	0.84	0	35.677	70	2.1	0	1.855	112	3.36	0	0	154	4.62	0	1	196	5.88	0	1
29	0.87	0	28.604	71	2.13	0	1.748	113	3.39	0	0	155	4.65	0	1	197	5.91	0	1
30	0.9	0	23.317	72	2.16	0	1.54	114	3.42	0	0.094	156	4.68	0	1	198	5.94	0	1
31	0.93	0	19.963	73	2.19	0	1.366	115	3.45	0	0.394	157	4.71	0	1	199	5.97	0	1
32	0.96	0	19.325	74	2.22	0	1.254	116	3.48	0	0.694	158	4.74	0	1	200	6	0	1
33	0.99	0	19.441	75	2.25	0	1.254	117	3.51	0	1.07	159	4.77	0	1				
34	1.02	0	19.608	76	2.28	0	1.254	118	3.54	0	1.281	160	4.8	0	1				
35	1.05	0	19.424	77	2.31	0	1.254	119	3.57	0	1.517	161	4.83	0	1				
36	1.08	0	19.193	78	2.34	0	1.254	120	3.6	0	1.674	162	4.86	0	1				
37	1.11	0	18.16	79	2.37	0	1.254	121	3.63	0	1.589	163	4.89	0	1				
38	1.14	0	16.131	80	2.4	0	1.089	122	3.66	0	1.558	164	4.92	0	1				
39	1.17	0	13.096	81	2.43	0	0.813	123	3.69	0	1.573	165	4.95	0	1				
40	1.2	0	9.805	82	2.46	0	0.599	124	3.72	0	1.573	166	4.98	0	1				
41	1.23	0	6.961	83	2.49	0	0.422	125	3.75	0	1.573	167	5.01	0	1				
42	1.26	0.	5.491	84	2.52	0	0.325	126	3.78	0	1.573	168	5.04	0	1				

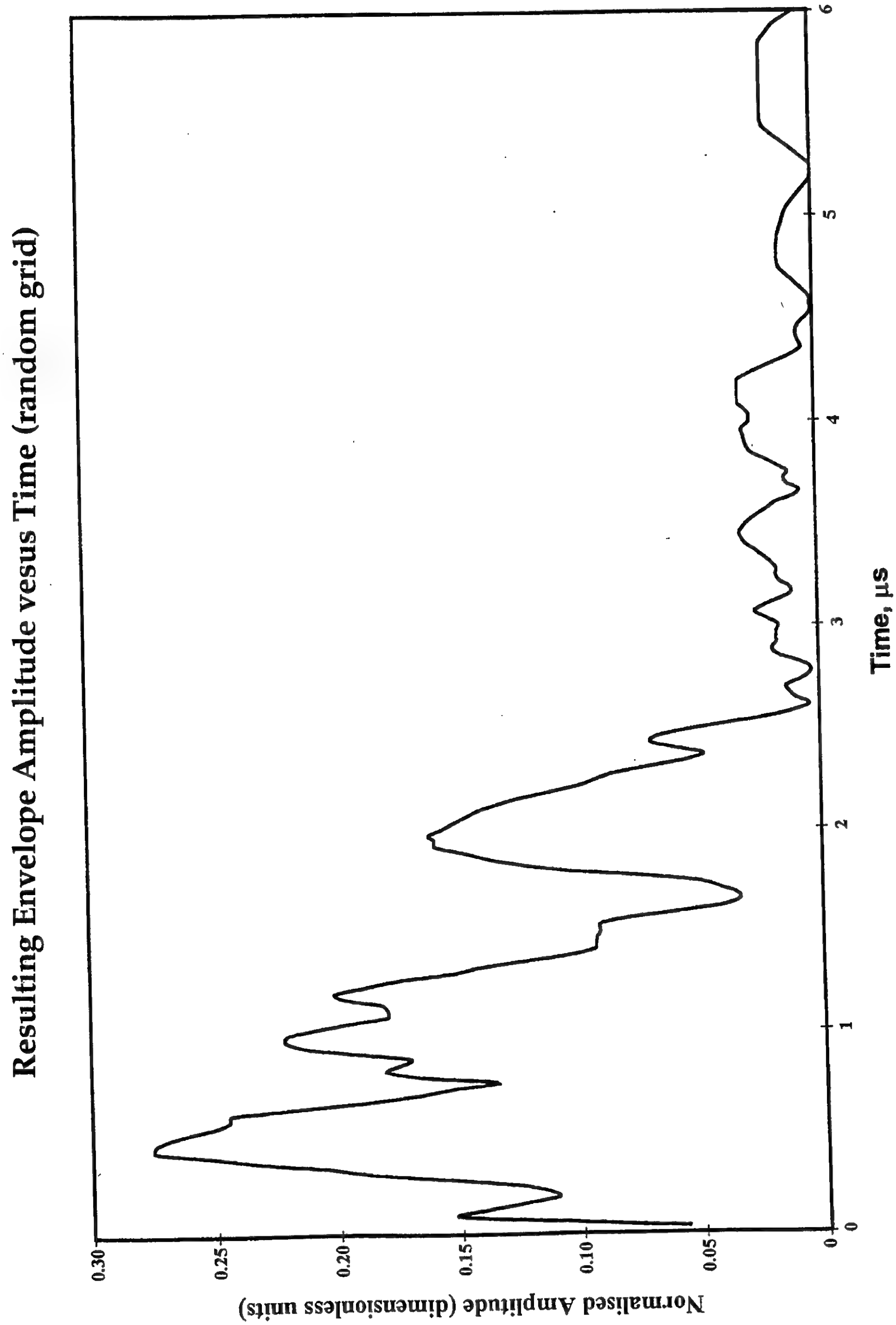
Resulting Envelope Amplitude vesus Time (random grid)
Normalised Amplitude (dimensionless units)
0.30
0.25
0.20
0.15
0.10
0.05
0
0
1
2
3
4
5
6
Time, µs

Beamwidth angle beta (degrees): 8
Great circle distance l (km): 300
Elevation angle phi (degrees): 4.1
Number of knots inside the scattering volume n: 1000
Operating frequency (MHz): 2830
Pulse rise time (μs): 0.1
Pulse width (μs): 0.5
Pulse fall time (μs): 0.15

i	Time[i]	Amplitude (arbitrary units)		i	Time[i]	Amplitude (arbitrary units)		i	Time[i]	Amplitude (arbitrary units)		i	Time[i]	Amplitude (arbitrary units)		i	Time[i]	Amplitude (arbitrary units)	
		Initial	Resulting			Initial	Resulting			Initial	Resulting			Initial	Resulting			Initial	Resulting
1	0.03	0.3	5.753	43	1.29	0	15.318	85	2.55	0	2.051	127	3.81	0	1.984	169	5.07	0	0.746
2	0.06	0.6	11.226	44	1.32	0	14.151	86	2.58	0	1.001	128	3.84	0	2.516	170	5.1	0	0.546
3	0.09	0.9	15.123	45	1.35	0	12.421	87	2.61	0	0.398	129	3.87	0	2.722	171	5.13	0	0.346
4	0.12	1	13.946	46	1.38	0	10.485	88	2.64	0	0.923	130	3.9	0	2.815	172	5.16	0	0.146
5	0.15	1	12.391	47	1.41	0	9.325	89	2.67	0	1.181	131	3.93	0	2.864	173	5.19	0	0
6	0.18	1	11.029	48	1.44	0	9.272	90	2.7	0	1.302	132	3.96	0	2.921	174	5.22	0	0
7	0.21	1	11.398	49	1.47	0	9.231	91	2.73	0	0.736	133	3.99	0	2.634	175	5.25	0	0.017
8	0.24	1	12.665	50	1.5	0	9.074	92	2.76	0	0.347	134	4.02	0	2.597	176	5.28	0	0.317
9	0.27	1	15.375	51	1.53	0	9.073	93	2.79	0	0.361	135	4.05	0	2.746	177	5.31	0	0.617
10	0.3	1	18.887	52	1.56	0	7.829	94	2.82	0	0.837	136	4.08	0	3.031	178	5.34	0	0.921
11	0.33	1	20.709	53	1.59	0	5.798	95	2.85	0	1.59	137	4.11	0	3.059	179	5.37	0	1.289
12	0.36	1	23.251	54	1.62	0	3.9	96	2.88	0	1.855	138	4.14	0	3.059	180	5.4	0	1.58
13	0.39	1	25.258	55	1.65	0	3.314	97	2.91	0	1.67	139	4.17	0	3.059	181	5.43	0	1.873
14	0.42	1	27.503	56	1.68	0	3.512	98	2.94	0	1.677	140	4.2	0	3.02	182	5.46	0	1.968
15	0.45	1	27.476	57	1.71	0	4.191	99	2.97	0	1.65	141	4.23	0	2.529	183	5.49	0	1.968
16	0.48	1	27.035	58	1.74	0	5.134	100	3	0	1.598	142	4.26	0	1.988	184	5.52	0	1.968
17	0.51	1	26.151	59	1.77	0	7.474	101	3.03	0	2.072	143	4.29	0	1.402	185	5.55	0	1.968
18	0.54	1	25.054	60	1.8	0	10.685	102	3.06	0	2.509	144	4.32	0	0.874	186	5.58	0	1.968
19	0.57	1	24.458	61	1.83	0	12.503	103	3.09	0	2.19	145	4.35	0	0.487	187	5.61	0	1.968
20	0.6	1	24.397	62	1.86	0	13.74	104	3.12	0	1.57	146	4.38	0	0.581	188	5.64	0	1.968
21	0.63	0.8	21.68	63	1.89	0	14.767	105	3.15	0	1.06	147	4.41	0	0.668	189	5.67	0	1.968
22	0.66	0.6	18.845	64	1.92	0	15.838	106	3.18	0	1.11	148	4.44	0	0.674	190	5.7	0	1.968
23	0.69	0.4	16.793	65	1.95	0	15.858	107	3.21	0	1.507	149	4.47	0	0.522	191	5.73	0	1.968
24	0.72	0.2	15.34	66	1.98	0	16.076	108	3.24	0	1.657	150	4.5	0	0.256	192	5.76	0	1.968
25	0.75	0	13.446	67	2.01	0	15.494	109	3.27	0	1.624	151	4.53	0	0.088	193	5.79	0	1.968
26	0.78	0	16.38	68	2.04	0	15.031	110	3.3	0	1.816	152	4.56	0	0.101	194	5.82	0	1.968
27	0.81	0	17.969	69	2.07	0	14.504	111	3.33	0	2.124	153	4.59	0	0.101	195	5.85	0	1.956
28	0.84	0	17.486	70	2.1	0	14.007	112	3.36	0	2.416	154	4.62	0	0.275	196	5.88	0	1.78
29	0.87	0	17.026	71	2.13	0	13.225	113	3.39	0	2.789	155	4.65	0	0.538	197	5.91	0	1.564
30	0.9	0	19.215	72	2.16	0	12.344	114	3.42	0	2.989	156	4.68	0	0.802	198	5.94	0	1.368
31	0.93	0	21.397	73	2.19	0	11.095	115	3.45	0	3.09	157	4.71	0	1.066	199	5.97	0	0.976
32	0.96	0	22.121	74	2.22	0	9.923	116	3.48	0	2.934	158	4.74	0	1.33	200	6	0	0.597
33	0.99	0	22.063	75	2.25	0	9.135	117	3.51	0	2.692	159	4.77	0	1.385				
34	1.02	0	20.891	76	2.28	0	8.407	118	3.54	0	2.339	160	4.8	0	1.385				
35	1.05	0	19.594	77	2.31	0	6.917	119	3.57	0	1.931	161	4.83	0	1.385				
36	1.08	0	17.93	78	2.34	0	5.493	120	3.6	0	1.589	162	4.86	0	1.385				
37	1.11	0	17.908	79	2.37	0	4.724	121	3.63	0	0.95	163	4.89	0	1.369				
38	1.14	0	18.162	80	2.4	0	5.805	122	3.66	0	0.86	164	4.92	0	1.293				
39	1.17	0	19.675	81	2.43	0	6.868	123	3.69	0	1.124	165	4.95	0	1.218				
40	1.2	0	20.099	82	2.46	0	6.6	124	3.72	0	1.25	166	4.98	0	1.144				
41	1.23	0	18.87	83	2.49	0	5.273	125	3.75	0	1.114	167	5.01	0	1.07				
42	1.26	0	17.475	84	2.52	0	3.603	126	3.78	0	1.5	168	5.04	0	0.946				

Prediction of Radar Pulse Envelope Distortion due to Tropospheric Propagation

Marina Oszerova

(DSTO-TN-0125)

AUSTRALIA

	Number of Copies
DEFENCE ORGANISATION	
S&T Program	
Chief Defence Scientist FAS Science Policy AS Science Corporate Management } shared copy	1
Director General Science Policy Development	1
Counsellor Defence Science, London	Doc Data Sheet
Counsellor Defence Science, Washington	Doc Data Sheet
Scientific Adviser to MRDC Thailand	Doc Data Sheet
Director General Scientific Advisers and Trials/ Scientific Adviser Policy and Command (shared copy)	1
Navy Scientific Adviser	Doc Data Sheet 1 x distribution list
Scientific Adviser - Army	Doc Data Sheet 1 x distribution list
Air Force Scientific Adviser	1
Director Trials	1
Aeronautical and Maritime Research Laboratory	
Director	1
Electronics and Surveillance Research Laboratory	
Director	1
Chief of Wide Area Surveillance Division	1
Chief of Electronic Warfare Division	1
Research Leader, RF Electronic Warfare	1
Research Leader, EO Electronic Warfare	1
Research Leader, System Integration & Operation	1
Head, Sensor Environment and Electromagnetics Group, WASD	1
Head, ES Systems & Technologies Group	1
Dr Andrew Kulessa, EWD	1
Dr Simon Rockliff,EWD	1
Marina Ozerova, WASD	1
Prof Doug Gray, University of Adelaide	1
DSTO Library	
Library Fishermens Bend	1
Library Maribyrnong	1
Library Salisbury	2
Australian Archives	1

Library, MOD, Pyrmont	Doc Data sheet
Capability Development Division	
Director General Maritime Development	Doc Data Sheet
Director General Land Development	Doc Data Sheet
Director General C3I Development	Doc Data Sheet
Army	
ABCA Office, G-1-34, Russell Offices, Canberra	4
SO (Science), DJFHQ(L), MILPO Enoggera, Queensland 4051	Doc Data Sheet
NAPOC QWG Engineer NBCD c/- DENGRS-A, HQ Engineer Centre Liverpool Military Area, NSW 2174	Doc Data Sheet
Intelligence Program	
DGSTA Defence Intelligence Organisation	1
Corporate Support Program (libraries)	
OIC TRS, Defence Regional Library, Canberra	1
Officer in Charge, Document Exchange Centre (DEC)	1
US Defense Technical Information Center,	2
UK Defence Research Information Centre,	2
Canada Defence Scientific Information Service,	1
NZ Defence Information Centre,	1
National Library of Australia,	1
UNIVERSITIES AND COLLEGES	
Australian Defence Force Academy	
Library	1
Head of Aerospace and Mechanical Engineering	1
Senior Librarian, Hargrave Library, Monash University	1
Librarian, Flinders University	1
OTHER ORGANISATIONS	
NASA (Canberra)	1
AGPS	1
State Library of South Australia	1
Parliamentary Library, South Australia	1

OUTSIDE AUSTRALIA

ABSTRACTING AND INFORMATION ORGANISATIONS	
INSPEC: Acquisitions Section Institution of Electrical Engineers	1
Library, Chemical Abstracts Reference Service	1
Engineering Societies Library, US	1
Materials Information, Cambridge Scientific Abstracts, US	1
Documents Librarian, The Center for Research Libraries, US	1
INFORMATION EXCHANGE AGREEMENT PARTNERS	
Acquisitions Unit, Science Reference and Information Service, UK	1

Library - Exchange Desk, National Institute of Standards and Technology, US	1
SPARES	10

Total number of copies: 62

Page classification: UNCLASSIFIED

DEFENCE SCIENCE AND TECHNOLOGY ORGANISATION DOCUMENT CONTROL DATA					1. PRIVACY MARKING/CAVEAT (OF DOCUMENT)
2. TITLE Prediction of Radar Pulse Envelope Distortion due to Tropospheric Propagation			3. SECURITY CLASSIFICATION (FOR UNCLASSIFIED REPORTS THAT ARE LIMITED RELEASE USE (L) NEXT TO DOCUMENT CLASSIFICATION) Document (U) Title (U) Abstract (U)		
4. AUTHOR(S) Marina Ozerova			5. CORPORATE AUTHOR Electronics and Surveillance Research Laboratory PO Box 1500 Salisbury SA 5108		
6a. DSTO NUMBER DSTO-TN-0125	6b. AR NUMBER AR-010-403		6c. TYPE OF REPORT Technical Note		7. DOCUMENT DATE December 1997
8. FILE NUMBER U 9505-13-146	9. TASK NUMBER DST 95/265	10. TASK SPONSOR DSTO	11. NO. OF PAGES 45		12. NO. OF REFERENCES 05
13. DOWNGRADING/DELIMITING INSTRUCTIONS			14. RELEASE AUTHORITY Chief, Electronic Warfare Division		
15. SECONDARY RELEASE STATEMENT OF THIS DOCUMENT Approved for Public Release OVERSEAS ENQUIRIES OUTSIDE STATED LIMITATIONS SHOULD BE REFERRED THROUGH DOCUMENT EXCHANGE CENTRE, DIS NETWORK OFFICE, DEPT OF DEFENCE, CAMPBELL PARK OFFICES, CANBERRA ACT 2600					
16. DELIBERATE ANNOUNCEMENT No limitations.					
17. CASUAL ANNOUNCEMENT	Yes				
18. DEFTEST DESCRIPTORS Tropospheric propagation Radar pulses Envelopes Distortion Radar signals					

19. ABSTRACT

This project is a part of research into the detection of radar signals at ranges well beyond the horizon by exploiting the effect of tropospheric scattering. A result of this work is a program written in C language which enables the distortion of the envelope of a given radar pulse, which occurs as a result of propagating over any path by tropospheric scattering, to be predicted.

Page classification: UNCLASSIFIED